CHARACTERIZATION AND EVALUATION OF A PROTOTYPE FORWARD-LOOKING AUTOMOTIVE RADAR (FLAR)

FINAL REPORT

NOTE TO READER:

THIS IS A LARGE DOCUMENT

Due to its large size, this document has been segmented into multiple files. All files separate from this main document file are accessible from links (blue type) in the table of contents or the body of the document.

654 100-9-F

CHARACTERIZATION AND EVALUATION OF A PROTOTYPE FORWARD-LOOKING AUTOMOTIVE RADAR (FLAR)

FINAL REPORT

SEPTEMBER 1997

R.K. Gilbert
P.K. Zoratti
R. Becker
G. Brumbaugh
T. Chaplin
M. Harrison
M. Hawks
K. Gondoly

Prepared for:
National Highway Traffic
Traffic Safety Administration
Office of Crash Avoidance Research
NRD-5 1, Room 6220
400 Seventh Street S.W.
Washington, D.C. 20590

Contract Number: DTNH22-94-Y-17016

P.0. Box 134008 Ann Arbor, MI 48113-4008 313-994-1200
http://www.erim-int.com

ERIM-320

REPORT DOCUMENTATION PAGE

Form Approved
OMB No. 0704-0188

1. AGENCY USE ONLY *(LeaveBlank)*	2. REPORT DATE	3. REPORT TYPE AND DATES COVERED
	March 1997	Final, from 1 March 1994 through 28 February 1997

4. TITLE AND SUBTITLE
Characterization and Evaluation of a Prototype Forward-Looking Automotive Radar Final Report

5. FUNDING NUMBERS
DTNH22-94-Y- 17016

6. AUTHOR(S)

R.K. Gilbert, P.K. Zoratti, R. Becker, G. Brumbaugh, T. Chaplin, M. Harrison, M. Hawks, and K. Gondoly

7. PERFORMING ORGANIZATION NAME(S) AND ADDRESS(ES)

Environmental Research Institute of Michigan (ERIM)
P.O. Box 134001
Ann Arbor, MI 48 113-4001

8. PERFORMING ORGANIZATION REPORT NUMBER
654100-9-F

9. SPONSORING/MONITORING AGENCY NAME(S) AND ADDRESS(ES)
National Highway Traffic Safety Administration
Office of Crash Avoidance Research
NRD-51 , Room 6220
400 Seventh Street, S.W.
Washington, D.C. 20590

10. SPONSORING/MONITORING AGENCY REPORT NUMBER

11. SUPPLEMENTARY NOTES

12a. DISTRIBUTION/AVAILABILITY STATEMENT
Limited Distribution

12b. DISTRIBUTION CODE

13. ABSTRACT *(Maximum 200 words)*

This is the final report for a three-year Discretionary Cooperative Agreement with the National Highway Traffic Safety Administration (NHTSA Grant DTNH22-94-Y-17016), "Characterization and Evaluation of a Forward-Looking automotive Radar Sensor." The Environmental Research Institute of Michigan (ERIM) and TRW were the industrial partners in this Cooperative Agreement. The goal of this research program was to increase the knowledge and understanding of radar sensing in the roadway environment by conducting structured testing of TRW's prototype automotive radar sensor, or FLAR, in real-world freeway settings. To achieve this goal, the following program objectives were established:

- to fully characterize TRW's FLAR in a controlled laboratory setting
- to measure radar cross-sections of representative automobiles and roadway objects
- to measure the performance of the FLAR in a variety of freeway settings
- to provide data to TRW for refining its prototype sensor design
- to begin developing methodologies to test, evaluate, and certify sensors for collision avoidance system

14. SUBJECT ITEMS
Automotive Radar Sensor, FLAR, Collision Avoidance System

15. NUMBER OF PAGES

16. PRICE CODE

17. SECURITY CLASSIFICATION OF REPORT	18. SECURITY CLASSIFICATION OF THIS PAGE	19. SECURITY CLASSIFICATION OF ABSTRACT	20. LIMITATION OF ABSTRACT
UNCLASSIFIED	UNCLASSIFIED	UNCLASSIFIED	Same as report

CONTENTS

CONTENTS (CONTINUED)

FIGURES

FIGURES (CONTINUED)

FIGURES (CONTINUED)

FIGURES (CONTINUED)

TABLES

1.0 EXECUTIVE SUMMARY

This document is the final report for a three-year Discretionary Cooperative Agreement with the National Highway Traffic Safety Administration (NHTSA Grant DTNH22-94-Y-17016), "Characterization and Evaluation of a Forward-Looking Automotive Radar Sensor." The goal of this research program was to increase the knowledge and understanding of radar sensing in the roadway environment by conducting structured testing of TRW's prototype forward-looking automotive radar sensor, or FLAR, in real-world freeway settings. To achieve this goal, the following program objectives were established:

- to fully characterize TRW's FLAR in a controlled laboratory setting,
- to measure radar cross-sections of representative automobiles and roadway objects,
- to measure the performance of the FLAR in a variety of freeway settings,
- to provide data to TRW for refining its prototype sensor design, and
- to begin developing methodologies to test, evaluate, and certify sensors for collision avoidance systems.

The findings and recommendations from this research program have national significance from several perspectives, including improved traffic safety and increased competitiveness of the United States Intelligent Transportation System (ITS) industry. The successful deployment of effective sensor-based systems obviously requires a foundation of reliable and low-cost enabling technologies. These results can be used by NHTSA to further its understanding of currently available technologies and to assess system reliability in benefits analyses for crash-avoidance applications. Finally, the radar supplier can use the results of this research effort to further the commercial development of these sensor technologies (Thrust Number 4 of NHTSA's Five-Thrust ITS Strategy).

The various results of this research effort are available in the following:

- This final report summarizes all of the results of the program including discussions of the roadway tests.
- The "Catalog of Radar Scattering Characteristics for Common Roadway Objects" contains radar cross-section plots and images for a number of different objects.
- The raw radar cross-section data is also available for downloading from the ERIM Web server: www.erim.org/Trans/roadobj/.

The key results and conclusions for the program are now briefly summarized.

1.1 CHARACTERIZATION OF VEHICLES AND ROADWAY OBJECTS

This program established an initial database for the radar scattering characteristics of a number of common roadway objects. This database begins to define the environmental framework in which an automotive radar must operate. Under this program four different "classes" of vehicles were characterized along with a motorcycle, human, stop sign, and cinder block wall.

Radar data for each object was collected using a 94 GHz Inverse Synthetic Aperture Radar (ISAR) test facility. The ISAR supported the creation of two-dimensional images for each object at a number of different aspect angles. The aspect angle refers to the relative orientation between the radar and the object. For example, a 0 degree aspect angle of a vehicle corresponds to viewing the vehicle head-on with the radar and a 180 degree aspect angle corresponds to viewing the vehicle from the rear. The two-dimensional images are color-coded to indicate intensity of the radar returns caused by each section of the object.

These images are useful in identifying the various radar scattering attributes of the object. For example, the impact of side-view mirrors, wheel housings, under-body structures, and body panel seams is evident in the images. Knowledge of the distribution of radar scattering centers across various objects could prove to be beneficial to radar processing and threat assessment algorithm developers.

In addition to the images, the characterization procedure produced radar cross-section (RCS) values for each object. The RCS is a quantitative value related to the object's level of radar reflectivity. The RCS of each object can be analyzed as a function of aspect angle or a function of range across the object.

For the objects characterized in this program, it was observed that the RCS value can range from a maximum of approximately +40 dBsm for a 90 degree aspect angle of a Jeep Wrangler, down to -10 dBsm for a 45 degree aspect angle of a stop sign. The primary factors which account for an object's RCS level are the material from which the object is made, the aspect angle between the radar and the object, and the geometric shape of the object. Square objects with flat surfaces, such as a Jeep Wrangler or a cinder block wall, exhibited relatively sharp peak RCS values for aspect angles which resulted in specular returns and much lower returns for aspect angles which deviated from specular orientations. On the other hand, more rounded objects such as a Geo Metro or a human being resulted in RCS values which were not as dependent on aspect angle.

The RCS data is critical in defining the dynamic operating envelope of the radar sensor. For example, from the measurements made in this program, it can be concluded that to detect a human being within its field-of-view, the radar sensor must have enough sensitivity to identify returns from an object with an RCS of around -5 dBsm at the systems desired operating range. Furthermore, the radar sensor must maintain this level of sensitivity when an object with a +40 dBsm RCS is also located within the radar field-of-view.

1.2 ROADWAY TESTS

The FLAR sensor was subjected to a number of orchestrated and non-orchestrated tests for evaluating its performance under a variety of roadway scenarios. The primary focus of these tests was to evaluate how the radar sensor itself interacted with the roadway environment. The TRW FLAR sensor was designed for an Adaptive Cruise Control (ACC) application, and therefore care must be taken in differentiating between the raw radar sensor performance and the TRW processing performance associated with the ACC application. To effectively evaluate the radar sensor, TRW provided access to the raw intermediate frequency (IF) radar signal prior to any TRW processing of the data. This allowed the raw radar data corresponding to any specific roadway scenario to be captured for subsequent processing and analysis.

To support the roadway data analysis, ERIM developed a testbed vehicle with data acquisition capabilities and a data playback software tool. The testbed vehicle provided a means of collecting raw radar data, TRW-processed radar data (range, range rate, etc.), video of the roadway, and vehicle position data from a GPS receiver. The GPS position data was combined with position data from other vehicles to serve as a "truthing" mechanism to assess the accuracy of the FLAR sensor. All of the data was collected and stored for each test scenario. The data playback software was then used to review the data and identify areas for further processing and analysis.

The roadway collections were designed to address some pre-defined sensing scenarios of concern, such as background induced false alarms, vehicle clutter induced falser alarms, tracking as a function of roadway geometry, and tracking in dynamic traffic of varying density. Appendix E of this report contains the program test plan.

Post-collection processing and analysis identified several scenarios as being potentially problematic for the FLAR sensor in terms of generating false alarms or missed detections. These scenarios are summarized below:

- **Roadside vehicles on a straight roadway** were observed to generate-returns in the raw radar data at certain geometries which could be interpreted as objects within the host vehicle's lane.
- **Adjacent lane vehicles on a straight roadway** viewed by the FLAR side beam antennas can generate multiple returns with significant range separation.
- **Guard rails and other roadside objects on curved roadways** generated significant returns which could cause false alarm problems.
- **Tracking vehicles around curved roadways** could prove to be problematic without knowledge of the roadway geometry in front of the sensor.
- **Near-range cut-ins and tracking of narrow vehicles** such as motorcycles could cause missed detections due to limited radar field-of-view.
- **Low RCS vehicles located between radar and large RCS** vehicles could cause missed detections.
- **Bridge or other roadway** overpasses were observed to generate significant returns in the raw radar data under certain circumstances.

In general, the radar sensor itself performed very well in the roadway tests. Somewhat counter-intuitive was the fact that the FLAR performed better under heavier traffic densities than under very light traffic densities. The response time of the raw radar data signal was virtually instantaneous. Two areas of the sensor system design were identified as critical to achieving adequate roadway performance: (1) antenna design and control, and (2) receiver gain control.

1.3 TESTING, EVALUATION AND CERTIFYING METHODOLOGIES

In addition to increasing the general knowledge and understanding of radar sensing in the roadway environment, the FLAR program has established empirical data and identified procedures to support the development of methodologies to test, evaluate, and certify sensors for collision avoidance/warning and adaptive cruise control systems. The program has identified three primary levels at which the testing should occur:

1. Laboratory testing to characterize and baseline the sensor's performance.
2. Environmental testing to identify the range of conditions under which the sensor can perform effectively.
3. Controlled roadway testing to verify algorithmic robustness in specific scenarios of interest to the intended application.

The objective of the laboratory characterization is to validate the standard performance specifications of the sensor. These specifications include ranging accuracy, range rate accuracy, range resolution, transmitted power, and field-of-view. The accuracy and stability of these performance specifications are innately linked to the sensor electronic circuitry. For example, it was discovered during the characterization of the FLAR sensor that the modulation rate was not exactly equal **to** that specified. This error was manifested in a reported "range to target" error which increased with higher ranges. It will be necessary for some quality control inspection of manufactured sensors to be performed to verify fundamental electronic performance. This is especially critical since the cost constraints for automotive-based equipment forces tradeoffs in sensor design and circuitry utilization.

The objective of the environmental testing is to identify sensor performance degradation susceptibility in terms of precipitation interference, material occlusion, and radome/target contamination.

Precipitation tests conducted with the FLAR sensor showed that 94 GHz energy was only marginally affected by various types of airborne precipitation (e.g., rain, snow, and fog). In particular, the precipitation did not induce any observable return levels in the raw radar data, and the attenuation levels were low (in most cases <1 dB/10 m for two-way travel). Of course these attenuation levels are dependent upon precipitation density and particulate size. The most significant outcomes of the precipitation tests were that the radar detected objects within its field-of-view even though the objects were partially or totally visually obscured. Furthermore, material tests indicated that while items such as plastic and glass may cause significant attenuation, 94 GHz energy does exhibit material penetration capabilities which will allow for concealment of the sensor within the automobile structure. The key to environmental testing is to insure that the sensor system operates appropriately under all likely conditions, or that the system can detect when its ability to perform has deteriorated and notify the operator.

The objective of the "controlled" roadway testing is to validate operation at a systems level. This takes into account not only the raw sensor performance, but also the processing and threat assessment or vehicle tracking algorithms for the ACC and CWS applications. This program has identified a number of scenarios which could prove to be problematic for an automobile-based radar sensor. The scenarios which have been cited are by no means exhaustive, but they do provide a starting point around which specific standard testing procedures can be developed. Repeatability of these standard testing procedures is necessary to allow both developers and OEM's to verify acceptable system operation under the same conditions. The vision of this testing process is to define a roadway scene in terms various objects, vehicles, and calibrated radar reflectors positioned to recreate a real-world roadway scenario of interest. The host vehicle can then drive a predetermined trajectory through this scene and the sensor system performance can be evaluated. Both the roadway and RCS data collected as part of this FLAR program will support the definition of the standard roadway scenes discussed above.

1.4 CONCLUDING REMARKS AND SUGGESTED FUTURE EFFORTS

In summary, this FLAR program has:

- Increased the general knowledge and understanding of vehicle-based radar sensing of the roadway environment.
- Established a radar cross-section database for a number of common roadway objects. This database begins to defme the operational envelope in which a vehicle-based radar sensor must operate. The database also supports advance simulation of the roadway environment.
- Identified a number of roadway scenarios which could be problematic for a vehicle-based sensor system. Empirical data on these scenarios will support the creation of standardized repeatable roadway testing procedures.
- Evaluated the weather performance and material penetration characteristics of a 94 GHz radar sensor.
- Established criteria for the baseline characterization and testing of the vehicle-based radar sensors.

The program results are available to interested parties in the form of this final report, an RCS catalog, and data on the world-wide web.

The results of this program serve to aid system developers and evaluators in terms of a more clearly defined operating environment and criteria for meaningful testing procedures. However, the successful deployment of radar technology in vehicle-based applications requires more work in many areas including:

. Mutual Interference Issues

- Manufacturing, Installation, and Calibration Issues
- Use of Simulation to Refine Sensor Design and Algorithm Implementation
- Human Factors and Response to Nuisance Alarms
- Human Factors and Response to Avoidance Maneuvers

2.0 INTRODUCTION

The goal of this research program was to increase the knowledge and understanding of radar sensing in the roadway environment by conducting structured testing of TRW's prototype automotive radar sensor, or FLAR, in real-world freeway settings. To achieve this goal, the following program objectives were established:

- to fully characterize TRW's FLAR in a controlled laboratory setting,
- to measure radar cross-sections of representative automobiles and roadway objects,
- to measure the performance of the FLAR in a variety of freeway settings,
- to provide data to TRW for refining its prototype sensor design, and
- to begin developing methodologies to test, evaluate, and certify sensors for collision avoidance systems.

The results and findings from this research effort are summarized by program objective. Feedback to TRW regarding the performance of its FLAR was provided throughout the program, and was not executed as a specific task. Testing and evaluation methodologies were addressed as part of each testing task. The Annual Reports provide a chronological summary of the Program's activities over the first two years. The third year was dedicated to roadway testing. Most of the test data, results, and supporting information can be found in the appendices.

2.1 TRW FORWARD-LOOKING AUTOMOTIVE RADAR (FLAR)

TRW provided two prototype automotive radars and technical support for test and evaluation. The first prototype, a single-beam radar, was only used during the first year of the program. At the start of the second year, TRW provided a radar with a greater azimuth field-of-view and multiple beams within this field-of-view. The integration of this higher performing radar into the test program greatly enhanced the value of the experimental results. There was a cost, however. Roadway tests were delayed for almost one year because the data acquisition system to had to be changed significantly to accommodate the radar upgrades. ERIM conducted a characterization procedure on each radar sensor to baseline performance. Much of the characterization parameters served to verify TRW's measurements as well as indicate areas where design improvements could increase sensor performance. Section 4 of this report provides a discussion of the characterization procedures and a description of the FLAR's baseline performance.

2.2 MATERIALS AND THE ENVIRONMENT

The Materials Tests were performed in a controlled, off-roadway setting in which all the test objects were stationary. The intent was to quantitatively assess the effect on the quality of the received signal produced by the environment in which these systems will be deployed and by typical materials used in cars and roadway construction. Baseband, time-domain data [i.e., before any signal processing such as the Fast Fourier Transform (FFT)], were collected and stored for off-line analysis. The following materials were evaluated: glass, plastic composite, Plexiglas, cardboard, wood, and rubber. The environmental test conditions included dry, raining, snowing, fog, contamination of radome, and contamination of target. Test data is provided in Appendix B.

2.3 RADAR CROSS-SECTION

The rnauner in which vehicles and other roadway objects interact with electromagnetic energy emitted by a radar is characterized by the object's radar cross-section, or RCS. The radar model presented in Appendix A explains the role of RCS in the overall performance of a radar for this application. RCS measurements were included in this program for two reasons: (1) to provide diagnostic data to support the analysis and evaluation of roadway tests; and (2) to initiate the development of a radar signatures database. The results of this effort were presented at the SPIE Conference in 1995[1] and at a meeting of the AVCS Committee held during the 1996 Annual Meeting of ITS America. While the RCS portion of the FLAR program effort was relatively small, response to the data produced was quite high on the part of automotive sensor developers.

2.4 ROADWAY TESTS

The Roadway Tests were conducted in both structured (on test tracks) and unstructured (on freeways) settings. To support these tests a data acquisition and analysis system had to be developed, and then upgraded when the prototype radar was upgraded (see Appendix C). This system was demonstrated at the 1995 Annual Meeting of ITS America, and at the AVCS Committee Meeting and Vehicle Demonstrations held at the Transportation Research Center (TRC) Inc., in East Liberty, Ohio in August, 1996. In addition, a differential GPS system was developed (see Appendix D) as atruthing tool. The structured tests (see Appendix E) were conducted at the TRC in October and November, 1996 according to a test plan developed in cooperation with NHTSA. The detailed test results of the structured test can be found in Appendix F and results from the unstructured tests found in Appendix G.

2.5 SUMMARY

This final report concludes with a summary of our findings, conclusions, and recommendations, focused on the use of a forward-looking radar for Adaptive Cruise Control Applications.

1"Millimeter Wave Scattering Characteristics and Radar Cross Section Measurements of Common Roadway Objects," P.K. Zoratti, J.J. Ference, R. Majewski, and R.K. Gilbert, SPIE Proceedings on Collision Avoidance and Automated Traffic Management Sensors, Vol. 2592, Philadelphia, PA, 25-26 October 1995.

3.0 MEASUREMENT OF TARGET CHARACTERISTICS/SIGNATURES

3.1 INTRODUCTION

This section summarizes ERIM's activities and findings for Task 3: Measurement of Target Characteristics/Signatures. The objective of Task 3 was to measure the radar scattering characteristics (e.g., the radar cross-section, or RCS) of representative roadway objects, using ERIM's Fine Resolution Rotary Platform Imaging Facility. This imaging approach is valuable because it provides system developers not only with calibrated radar data, but also with two-dimensional radar images. From these, information about individual point scatterers within a single target can be extracted. This information on scattering characteristics can be used to refine processing algorithms for threat assessment, guide the design of automotive radar hardware, and supplement automotive radar simulation programs.

To create a database of radar scattering characteristics for roadway objects, radar data was collected for the following objects:

- 1990 Chevy Corvette ZR-1
- 1995 Ford Taurus
- 1991 Jeep Wrangler
- 1993 Geo Metro EFI
- Honda Motorcycle
- 180 lb. person
- Stop Sign with a square post
- Cinder Block Wall

The entire set of data collected on these objects has been processed and organized into a "Catalog of Radar Scattering Characteristics for Common Roadway Objects." The NHTSA-OCAR has a version of this catalog containing black-and-white images. A catalog with full color images is available from ERIM at a nominal price to cover reproduction costs. Also, the data which constitutes the plots in the catalog can be downloaded from ERIM's Web server: www.erim.org/Trans/roadobj/.

The remainder of this section will discuss:

- background on the need for radar scattering characteristic data;
- methods for making the radar measurements;
- techniques for reducing the measurements to RCS data; and
- general descriptions of the various data output products, with guidelines for interpreting the data.

The section concludes with some general observations and conclusions based on the RCS data. This includes summary information on the variation of return levels and the RCS dependency on aspect angle.

3.2 BACKGROUND

Well-characterized radar RCS data will be essential for developing the guidelines and standards that will affect all phases of a radar-based product's lifecycle, from inception through installation on a vehicle. It begins with the design of both the hardware and the signal processing algorithms, includes methodologies for test and evaluation, and finally, certification that the devices meet specific

performance standards. The need for performance certification will be driven by the need to provide some legal protection against liability claims. At some point, crash avoidance systems will be offered to the public as features that wil1 make the automobile safer to operate. The possible causes for a "failure" are many, and suppliers will want a basis for demonstrating that their products perform as advertised.

This Radar Signatures Database is a mechanism for sharing information. As it is developed, it will eliminate redundant measurement activities on the part of developers to make their own measurements. This should reduce development costs, which in turn should reduce time-to-market and cost to the consumer.

For a given radar, the return from a roadway object will vary as a function of many parameters. These parameters include, but certainly are not limited to, the range and azimuth angle to the target, the target's geometry and materials, the weather, and surrounding roadway environment, which includes other vehicles and non-moving roadway objects. Each of these parameters can take on many values. The problem is further compounded by the number of radar parameters that can be varied. This literally results in a combinatoric explosion in the number of possible test conditions. Clearly such a problem must be approached in a structured and orderly manner. Creation of the Radar Signatures Database will be one method for bringing this problem under control.

3.3 RADAR MEASUREMENTS

The data for the Radar Signatures Database were collected on ERIM's Fine Resolution Rotary Platform Facility. The radar system is based on an HP85 10 Network Analyzer. The objective of the RCS collection task was to collect 94 GHz radar data for a number of roadway objects at various aspect angles. ERIM's Rotary Platform Facility (RPF) was well suited for the task. The RPF consists of a radar antenna pedestal mounted on the outside wall of ERIM's building and 22-foot diameter turntable located 135 feet from the pedestal. The turntable is capable of supporting up to 20,000 lbs and provides a convenient way to vary target aspect angles.

There are two important issues regarding the RCS measurements. The first deals with near-field/far-field effects. Radar cross section (RCS) is normally defined when the incident radar wave is a plane wave; consequently, RCS is normally a "far-field" RCS. The normal requirement for being in the far-field is that the phase deviation from planar is less than 22.5 degrees which translates to a range of at least $2D^2/h$ where D is the target diameter and h is the wavelength. For example, a target with a 2-meter diameter being illuminated by a 77 GHz radar would have to be 2053 meters away to be in the far-field; consequently, automotive radars certainly can operate in the "near-field" when considering objects the size of vehicles. With the collection set-up utilized on ERIM's RPF, the illumination pattern from the 94 GHz radar would be considered to be in the far-field (based on the size of the transmit antenna and range to the platform); however, scatterers which are larger than 0.2 meters may exhibit near-field reflection characteristics. For example, in the far-field, a simple target like a flat plate has a reflection characteristic with a $(\sin X/X)^2$ pattern. As the range to the flat plate decreases below the far-field range, the nulls in the pattern fill in and the sidelobes increase. The overall effect of operating in the "near-field" is that the RCS patterns are range dependent and not constant. The RCS measurements provided in this report correspond to a specific range (40 meters). This should not be considered a significant limitation in analyzing the data for peak return levels and aspect angle characteristics.

The second issue is related to the radar illumination frequency. The measurements were made at 94 GHz to correspond to the TRW FLAR unit operating frequency. The TRW FLAR design is based on military radar technology; however since the inception of this program, the FCC has approved the 76 to 77 GHz band for automotive radar applications. The question therefore arises as to what effect the change in frequency will have on the RCS measurements which were made. The frequency change from 77 to 94 GHz is only 22 percent, so the changes in the RCS pattern for a simple reflector such as a flat

plate will be minor. However, with a complex object like a vehicle, the RCS is the vector summation of the contributions from a large number of individual scatterers distributed across the target. These individual scattering centers act independently of one another and as the range to the object changes, the phases of the contributions from the individual scattering centers will be different for 77 and 94 GHz. The locations of the peaks and nulls of the RCS pattern will vary with frequency; however the mean value of the RCS will not change significantly, and essential characteristics of the target RCS will be the same.

3.3.1 Experimental Setup

Figure 3-l illustrates the physical set-up for the data collection. The Network Analyzer based radar operates in a linear-FM (chirp) pulse mode. The Network Analyzer creates a baseband signal with 2 GHz of bandwidth, centered at 10 GHz. This signal is then amplified and sent to the RF plate, where it is up-converted from a 10 GHz to a 94 GHz center frequency and radiated at the target on the rotary platform using a standard gain horn antenna. The standard gain horn has an approximately 9 degree azimuth beamwidth which illuminates the entire platform. Signals reflected back from the target to the radar are captured by the RPF's receiver and down-converted to baseband and input to the network analyzer. The radar system preserves both the amplitude and the phase of the reflected signals. This information is downloaded from the network analyzer to a PC-based data acquisition system via an IEEE-488 communications bus.

In addition to storing the radar data, the PC also interfaces with an optical shaft encoder mounted on the rotary platform. The turntable must be driven at a very slow speed (e.g., 0.02 degrees/sec), due to the low PRF of the HP8510 and high image resolution requirements. The shaft encoder allows the table position to be exactly correlated with the collected radar data.

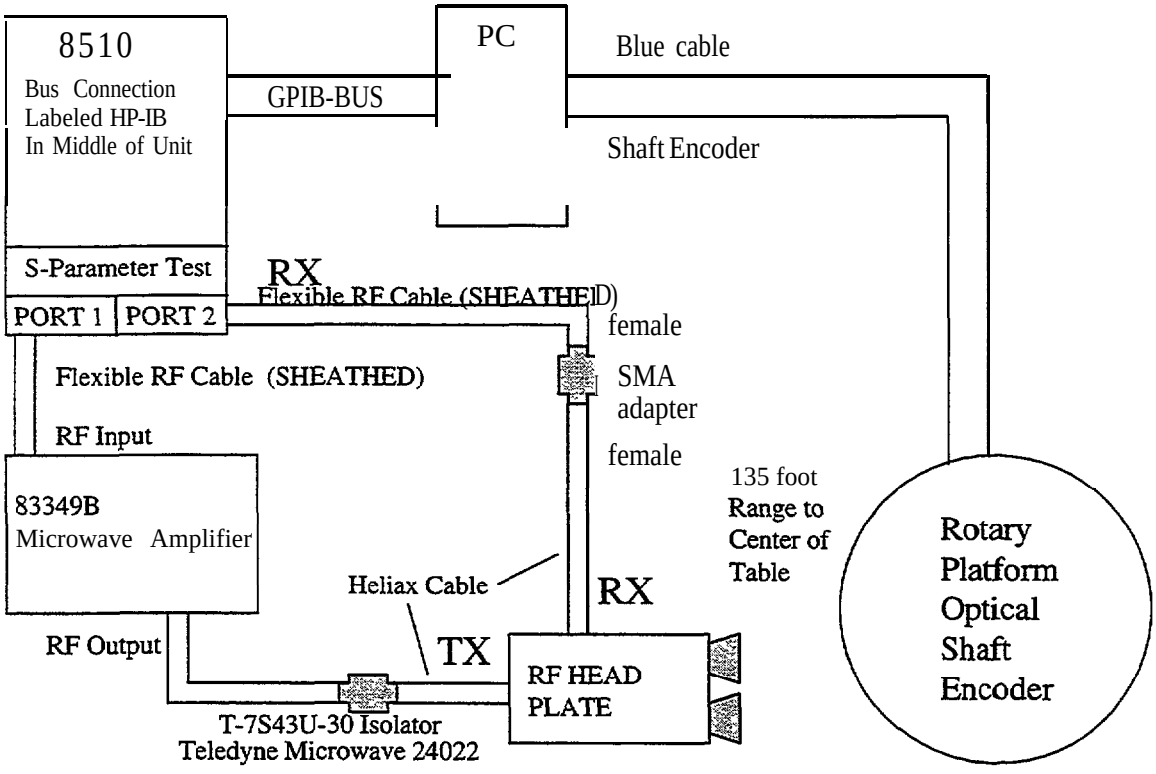

Figure 3-l. Data Collection Set-up

3.3.2 Data Collection

The table was rotated at a fixed rate to illuminate the objects from a continuum of aspect angles, so that Inverse Synthetic Aperture Radar (ISAR) processing techniques could be implemented, as described below, to produce fine azimuthal measurements of the target.

The radar collection system was calibrated prior to each measurement using a series of reference reflectors located on the platform. The reference reflectors have known radar cross-section (RCS) values. The calibration procedure produces a +3 dB accuracy across the rotary platform surface. Higher accuracies can be achieved by compensating for actual target range in the processing software, but this technique was not used here.

The vehicular objects and cinder block wall were located on the center of the table during the collection process. The human and the stop sign were located approximately 3 feet off-center to avoid any obscuration from stationary clutter fold-in. The surface between the collection radar and the rotary platform is fairly level, grass-covered ground. No multipath fences were employed during collections of the roadway objects, but they were used during the calibration procedure.

Table 3-1 summarizes the radar parameters used for these data collections.

Table 3- 1. Radar Parameters

Radar Parameter	Specification
Mode of Operation	Linear-FM Pulsed
Center Frequency	94 GHz
Bandwidth	2 GHz
Transmitted Power	@ 100 mW
Polarization	H/H
Pulse Repetition Frequency	@ 2 Hz

3.4 DATA PROCESSING

The collected radar reflections were downloaded from the collection PC to a Sun/UNIX workstation. The radar data (pulses) are floating point vectors that contain 801 arithmetically complex samples; that is, the samples have both a real and an imaginary part, which are thematically combined to represent the amplitude and phase of the radar returns.

The first processing operation suppresses the stationary clutter. Stationary clutter is energy reflected by all illuminated radar scatterers that were not a part of the rotating platform, such as the earth immediately surrounding the rotating table. To suppress the clutter, the processing software computes the coherent average of all pulses from the collection run. Because the energy reflected by scatterers on the platform averages approximately zero over the course of a complete platform rotation, the averaging operation produces an estimate of the return from only the stationary scatterers. The processing software then subtracts the average from each pulse, thereby suppressing the stationary clutter.

Following clutter suppression, the processing software performs a forward FFT on each pulse, mapping the data to the range-frequency (image) domain. The 801 samples cover a range swath that is about 60 meters wide. The center 120 samples are then extracted to provide a range subswath that is about 9 meters wide and centered on the platform. An inverse FFT is performed on the subset of 120 samples to map the data back to the time domain for subsequent processing.

The signal data next passes to the image formation processing software, where the image formation processor (IFP) produces two-dimensional images of the target by applying the polar format algorithm (PFA). The radar data could be processed directly into imagery with a two-dimensional FFT. However, FFT-based processing provides little control over image aspect ratio and it does not compensate the radar signal history for nonuniformities in the rotation rate of the platform. These nonuniformities can lead to azimuthal resolution variations in the final image. Because the PFA requires range and azimuth resampling of the signal history data, the processor provides the user with a ready mechanism for setting and maintaining both image resolution and aspect ratio.

The PFA also offers a mode of operation known as stabilized scene processing. Stabilized scene processing holds the orientation of the target constant from image to image, at an orientation angle specified by the user. When viewing a sequence of stabilized scene images, the radar appears to rotate around the target. Stabilized scene processing permits the processing software to form an additional output product known as a noncoherently integrated image, which is the sum of the magnitudes from a sequence of stabilized scene images. If the sequence of images covers 360 degrees of aspect angle change, the noncoherently integrated image will be a picture of the aggregate radar scattering of the illuminated target.

3.5 DATA OUTPUT PRODUCTS AND INTERPRETATION

Through informal discussions with parties interested in the RCS data, it became evident that the end-users would like the data processed and presented in a variety of ways. Therefore, we have created five different data output products:

1 Maximum Return Level versus Aspect Angle (Aspect Profile) Plot

2. Return Level versus Range (Range Profile) Plot

3. Two-Dimensional Image "Movie"

4. Two-Dimensional Image--Single Aspect Angle

5. Two-Dimensional Image--Integration of Multiple Aspect Angles

The following subsections describe these five data output products, how they should be interpreted, their potential utility, and current availability. Examples from the "Catalog of Radar Scattering Characteristics for Common Roadway Objects" are used in the explanation of each data type.

3.5.1 Maximum Return Level Versus Aspect Angle (Aspect Profile) Plot

Figure 3-2 is an example of a Maximum Return Level versus Aspect Angle Plot for the 1991 Jeep Wrangler. The aspect profile data indicates the maximum return level of the target as a function of aspect angle for a 360 degree rotation. The y-axis of the plot is the maximum return level (given in dBsm) for the corresponding aspect angle given on the x-axis. Note that the data reports the maximum return level, and not the total RCS of the object. The maximum return level corresponds to the highest power level observed in any given range cell (range cells for this data are approximately 7.5 cm). The maximum return levels are given in dBsm, corresponding to the radar cross-section of the most reflective scatterer on the object. Aspect angle values have been defined such that a 0 degree aspect angle corresponds to illuminating the object from a head-on orientation, a 90 degree aspect angle corresponds to illuminating the object from the left side (or driver side for a vehicle), a 180 degree aspect angle corresponds to illuminating the object from the rear, and a 270 degree aspect angle corresponds to illuminating the object from the right side (or passenger side for a vehicle)

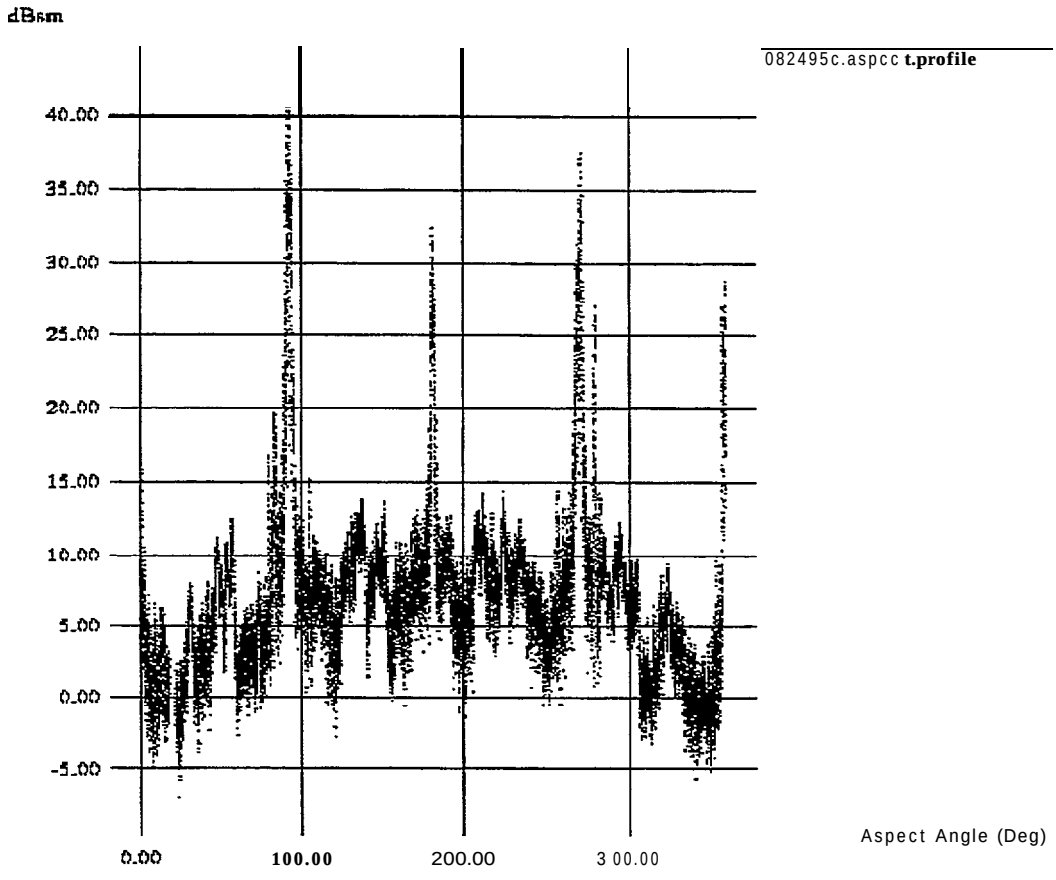

Figure 3-2. Example of Aspect Profile Plot

These data plots are useful for defining the dynamic operating envelope under which an automotive radar must operate. For example, the maximum return levels for the targets measured in this effort ranged from -12 dBsm (a stop sign at its lowest return aspect angle) to +42 dBsm (the Jeep at its highest return aspect angle). This means that the radar must be able to handle returns from targets of this size over its operating range. Another use for this type of data is in high-level simulation programs which do not require high fidelity in the radar models. One could use the data in these types of plots as a look-up table for expected reflectivity, given a specific aspect angle as generated under a particular scenario in the simulation program. The return level is provided in dBsm so that the user can scale expected power level returns according to individual radar configurations and range to target. The user should note, however, that since many automotive radars operate in the near-field, radar cross-section (RCS) is range dependent rather than constant (see Section 3.3).

These types of plots are available in both hard copy and electronic forms. Hard copies of these plots for each target are included in "Catalog of Radar Scattering Characteristics for Common Roadway Objects" which is provided as an appendix to this report in a black-and-white version. A color version is available from ERIM ($400). The data for these plots can also be downloaded at no charge from ERIM's Web server: www.erim.org/Trans/roadobj/.

3.5.2 Return Level Versus Range Plot (Range Profile) for a Given Aspect Angle

Figure 3-3 is an example of a Return Level versus Range Plot for the BMW motorcycle, at a 180 degree aspect angle. The y-axis of the plot is the return for the corresponding range given on the

x-axis. The return levels are given in dBsm, which corresponds to the radar cross-section of the scatterer(s) which constitute the return from that particular range. The range values correspond to the distance across ERIM's rotary platform table. The table itself is approximately 6.7 meters across. Therefore, a range of 0 corresponds to the edge of the platform nearest to the-radar, and a range 6.66 meters corresponds to the edge of the platform farthest from the radar. Each object (except the human and the stop sign) was positioned near the center of the table. Aspect angle values follow the definition provided in the previous section.

These types of data plots are useful for observing how the individual scatterers on the target are distributed as a function of range. Knowledge of scatterer distribution may be helpful in developing algorithms which group multiple scatterers together as a single target, to reduce the burden on tracking algorithms. Another use for this data type is in more advanced simulation programs which can utilize the range profiles to simulate targets at a given aspect angle in a particular scenario. The return level is provided in dBsm to allow the user to scale expected power level returns according to individual radar configurations and range to target, however the user should note that since many automotive radars operate in the near-field, radar cross-section (RCS) is range dependent, and is not constant.

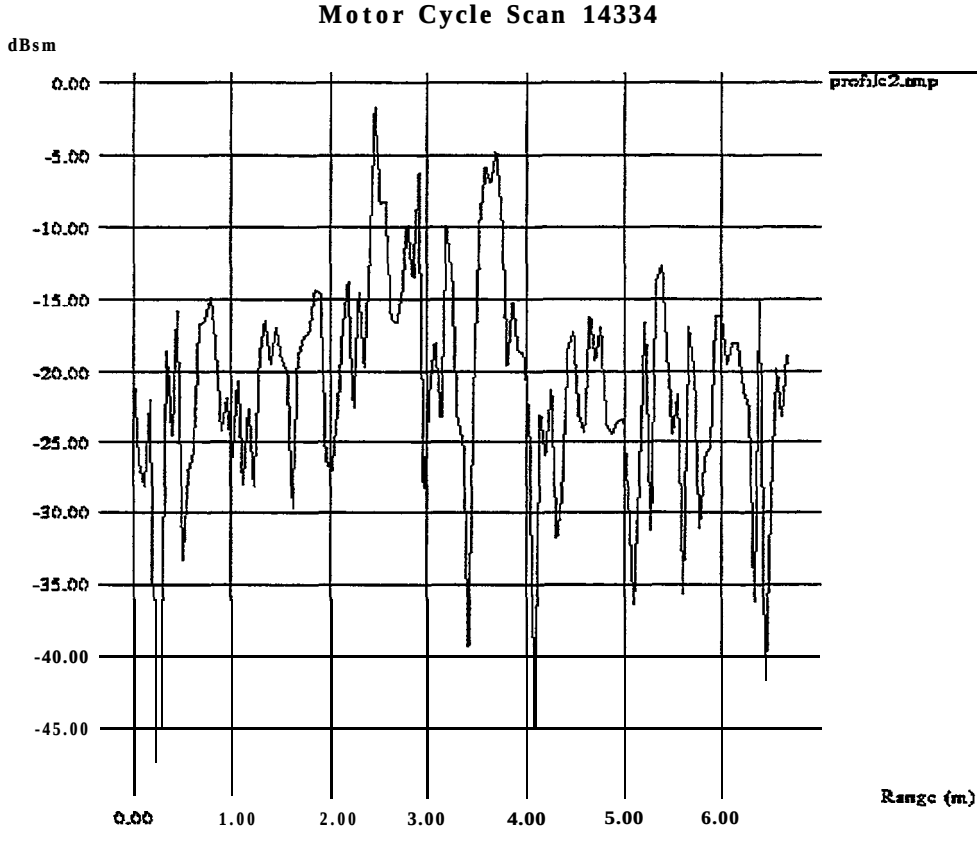

Figure 3-3. Example of Range Profile Plot

3.5.3 Two-Dimensional Image "Movie"

Since the radar data was collected and processed using Inverse Synthetic Aperture Radar (ISAR) techniques, a two-dimensional image of the illuminated object can be formed. A series of images can be linked together to create a dynamic "movie." The movie is a sequence of radar images taken at various

aspect angles and illustrates how the radar return levels vary as the vehicle is rotated. ERIM has a movie of a Ford Taurus available on its world-wide web server: www.erim.org/Trans/roadobj/.

The images in the movie are oriented such that the radar is illuminating from the right side and the observer is looking straight down at the vehicle. Therefore, range is in the horizontal direction and cross-range (i.e., azimuth) is in the vertical direction. The images in the movie are also color-coded, so that low level returns are represented by dark colors (e.g., blue and green) and higher Ievel returns are shown as brighter colors (e.g., orange and yellow). The movie indicates how very high-level returns occur when the front, rear, or sides of the vehicle are perpendicular to the radar illumination. This is due to specular (mirror-like) reflections of the radar energy. As the vehicle rotates away from the0,90, 180, or 270-degree aspect angles, the return levels drop off significantly.

Viewing the data in a movie-type format visually illustrates the dynamic changes in radar return levels with changing aspect angle. Aspect angles which correspond to low return levels can be easily identified for further analysis using the other forms of data output.

Production of these movies was achieved using ERIM's proprietary image manipulation software. Therefore, the movies are not publicly available. Organizations which have special requirements and are interested in viewing movies of other roadway objects can contact ERIM directly.

3.5.4 Two-Dimensional Image-Single Aspect Angle

Figure 3-4 shows black-and-white radar images and corresponding range profile plots of a 1990 Chevy Corvette at 170 and 180 degree aspect angles, respectively. The images are oriented such that the radar is illuminating from the left side and you are looking straight down at the vehicle. Therefore, range is in the horizontal direction and cross-range (i.e., azimuth) is in the vertical direction. The resolution cell of each image is approximately 7.5 by 7.5 centimeters. The images are coded with grey-shades to represent the radar return levels as designated in the scale on each image. The corresponding range profile plot is included below each image to illustrate how a vehicle-based radar might "view" this object.

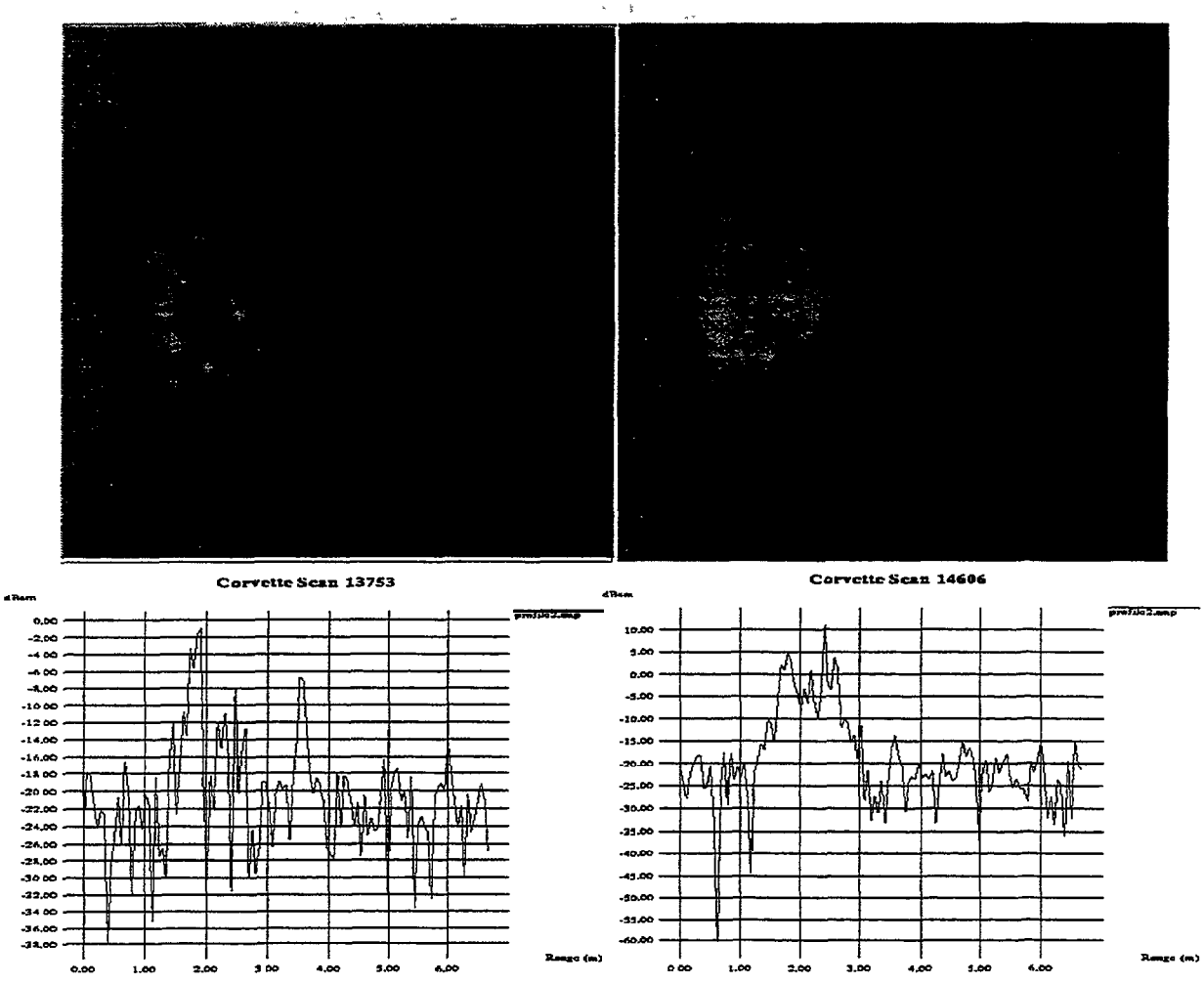

170 Degree Aspect Angle **180 Degree Aspect Angle**

Figure 3-4. **Examples of Single** Aspect Angle **Images**

These images allow the observer to identify individual scattering centers on the object which are active at a given aspect angle. This information can help to explain observations during static or roadway testing of vehicle-based radar sensors. For example, the range profile plot for the 180 degree aspect angle exhibits a "double hump" in the return which may puzzle some researcher. However, the image clearly shows that the second hump is due to a multipath return off the transmission housing underneath the vehicle.

3.5.5 Two-Dimensional Image--Integrated from Multiple Aspect Angles

A noncoherently integrated radar image of a 1993 Geo Metro is shown in Figure 3-5. This image was created by integrating the returns from multiple aspect images, like those discussed in the previous section, spaced at 5-degree increments. The image appears as though the object was being illuminated from all aspect angles simultaneously and you are looking straight down at the vehicle. Therefore, range is in the horizontal direction and cross-range (i.e., azimuth) is in the vertical direction. The resolution cell of the image is approximately 7.5 by 7.5 centimeters.

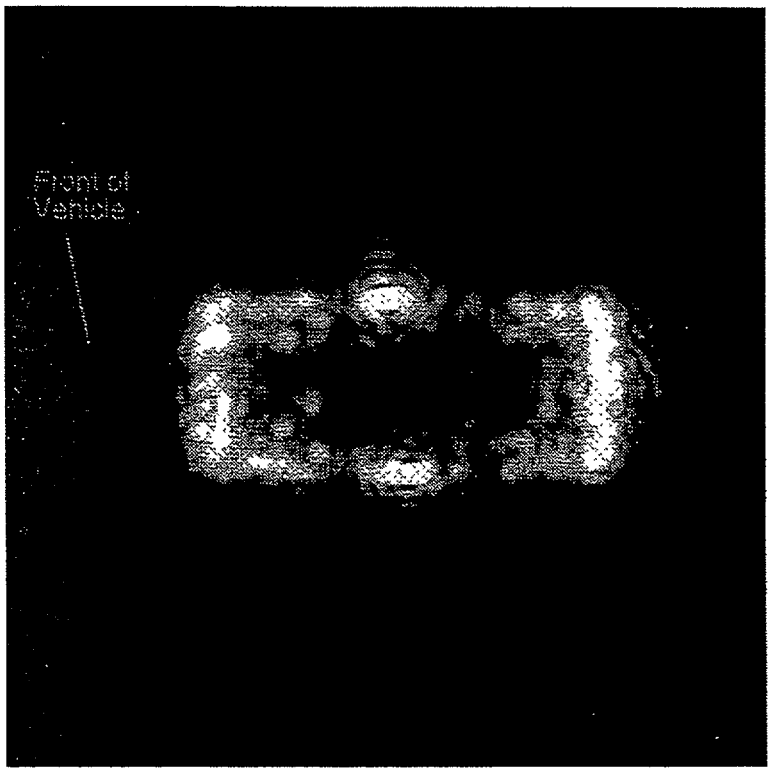

Figure 3-5. Example of Noncoherently Integrated Radar Image

The noncoherently integrated image allows the observer to identify all of the individual scattering centers on a given object. This information can help to explain observations during static or roadway testing of vehicle-based radar sensors. These types of images have been made for all of the vehicles on which data has been collected.

Hard copies of these plots for each target are included in "Catalog of Radar Scattering Characteristics for Common Roadway Objects" which is provided as an appendix to this report in a black-and-white version. A color version is available from ERIM ($400).

3.6 INITIAL OBSERVATIONS AND CONCLUSIONS

It is anticipated that the various data output products described above will find great utility in future automotive radar simulation programs and as guidelines for future designs and testing. Analysis of the RCS data has yielded a number of observations which will now be discussed.

Maximum and Minimum RCS Values

Observations of the RCS data indicate that reflectivity of common roadway objects can vary from over +40 dBsm for the broadside view of a Jeep-type vehicle to below -2 dBsm for a motorcycle or even -10 dBsm for an irregularly shaped sign post. This means that in order to detect these various objects in a given roadway scenario, the automotive radar must have a dynamic range greater than 50dB. In addition, the noise floor of the receiver must be low enough to reliably detect targets with RCS values as low as -5 to -10 dBsm at the maximum operating range of the system.

Return Levels From Aspect Angles Around 180 Degrees

Two of the primary applications of automotive radar will be for Intelligent Cruise Control purposes and for mitigating rear-end collisions. Therefore, the return levels from vehicles when illuminated from the rear (i.e., a 180 degree aspect angle) are critical. In evaluating the aspect profiles of the various vehicles measured in this effort, it was observed, as expected, that all of them except the motorcycle provided a significant return at 180 degrees due to specular reflections from the rear structure of the vehicles. It was also observed that as one deviated from the 180 degree view, the return level dropped off at various rates, based on the geometric shape of the vehicle. Table 3-2 shows the minimum angular departure from a 180 degree aspect at which the RCS of the vehicle drops below the specified value. For example, the reflectivity of a Taurus was observed to drop below 5 dBsm when the aspect angle was below 170 degrees or above 190 degrees.

Table 3-2. Characteristic RCS Fall-Off

Vehide	Angle of Departure From 180 at Which RCS >0 dBsm	Angle of Departure From 180 at Which RCS >5 dBsm	Angle of Departure From 180 at Which RCS >10 dBsm
Jeep	±180	±180	±5
Taurus	±20	±10	±5
Geo Metro	±40	±30	±5
Corvette	±30	±10	0
Motorcycle	±2	0	0

Looking at these numbers indicates that the reflectivity of certain classes of vehicles will drop below 0 dBsm at aspect angles which can be expected to be incurred during normal driving. Obviously the motorcycle poses the largest problem, but even the Taurus and the Corvette will fall below 0 dBsm in road curves. The effects of low RCS levels at common aspect angles will be tested during the road tests planned for this program.

Distribution of Scatterers Across Targets

The range profile plots, single aspect images, and radar image movies demonstrate that the radar energy scatterers are distributed across the extent of the target; they include side-view mirrors, wheels, under-body structures, in-vehicle components, body panel seams, and so forth. The relevance of this attribute to automotive radar is that tracking the returns from each individual scattering center will place an enormous burden on the radar processing and threat assessment electronics. The ability to group these returns into a single object is highly desirable. However, the RCS data indicates that this will not be a trivial task as the object's signature can change significantly with a minute change in aspect angle. This is due to the highly dynamic scintillation effects induced by the small wavelength of automotive radar energy. These effects were observed repeatedly during the roadway tests of this program, in which the returns from a vehicle being tracked by the FLAR varied over a wide range on a pulse-to-pulse basis.

Non-Vehicular Objects

One concern for automotive radars is the interpretation of returns from objects other than vehicles. These objects may be considered clutter if they are off to the side of the roadway (like a stop sign), or a legitimate threat (a pedestrian crossing the roadway). The RCS data collected under this program indicates that a human being can have a reflectivity between +4 and -6 dBsm. Stop signs have a large

specular return at a 0 degree aspect angle but can quickly fall below -5 dBsm. Also, like the stop sign, a block wall (used to simulate a bridge abutment) exhibits a large specular reflectivity which falls off rapidly as the aspect angle departs from 0 degrees.

Many more observations can be made from the data alone, but as mentioned above, the real utility of the data will be in its application for simulation programs. We expect to expand on this initial database during future projects.

It is interesting to note at this point that many of these conclusions, based on the analysis of the RCS data, were actually observed during the road testing phase of this program (see Section 6).

4.0 TRW FORWARD LOOKING AUTOMOTIVE RADAR (FLAR)

4.1 INTRODUCTION

Most of the radar testing in this program, excluding the RCS measurements of common roadway objects, was made using a TRW Forward Looking Automotive Radar (FLAR) The FLAR was provided by TRW and integrated into ERIM's testbed vehicle collection system. Its purpose was to serve as a "generic" automotive radar sensor and provide the basic signals from which ERIM could evaluate the interaction between the radar and its surrounding environment. It should be emphasized that the purpose of the experiments conducted in this program was NOT to test the hardware configuration or algorithms employed in TRW's design. On the contrary, the measurements were designed to isolate the results (as much as possible) from specific attributes of the TRW radar implementation.

This section will first describe the configuration and operation of the TRW radar and then present the results of basic tests conducted to determine baseline performance characteristics. These characteristics were used in subsequent roadway testing of the unit.

4.2 SENSOR CONFIGURATION

The TRW FLAR, model AICC-3B, utilizes 94 GHz radar technology originally developed for military purposes. The FLAR has 3 electronically switched transmit beams and 1 receive beam. Each transmit beam has 3 dB widths of 3 degrees in azimuth and 3 degrees in elevation. The receive beam is approximately 9 degrees in azimuth and 3 degrees in elevation. With this configuration, the sensor's field-of-view is adjusted by directing the signal to be transmitted to the appropriate transmit antenna.

The TRW AICC-3B FLAR consists of two elements (Figure 4-l): the RF head, which contains the transmit/receive antennas and the analog circuitry, and the DSP module which contains the processing unit and the interfaces to the host system (the test computer in the testbed vehicle). The DSP communicates to the RF head via three cables: one for the power connection, one for the radar data, and one for the beam selection bits. The DSP communicates with the host system via three cables: one cable for primary power and the other two for data communication.

In the ERIM testbed vehicle, the RF head is located on a hard mount in front of the vehicle grill, providing a field-of-view uncontaminated by any vehicle structural members. The DSP is located in the vehicle cabin along with the test computer rack.

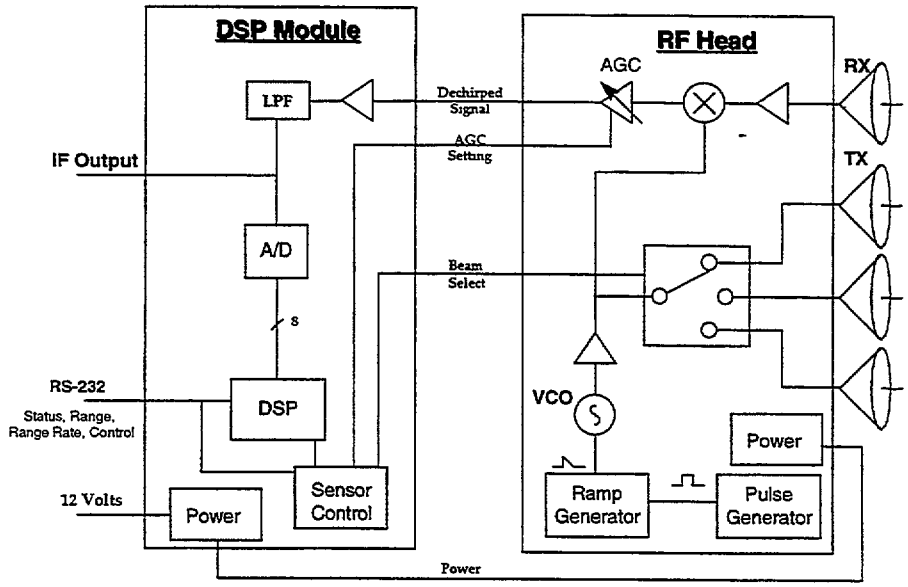

Figure 4-1. TRW's AICC-3B FLAR

4.3 SENSOR OPERATION

4.3.1 General Overview

The TRW FLAR employs a pulsed frequency-modulated, continuous wave (FMCW) radar front-end to determine the distance to objects located in its field-of-view (FOV). A high-level functional block diagram of the TRW radar sensor is shown in Figure 4-1. The following sequence of events describes the process to generate, transmit, and receive a single radar pulse:

1. The pulse generator within the RF head generates a modulation signal which dictates the fundamental timing of the radar.
2. The modulation signal (a square wave) drives the ramp generator, which creates a linearized voltage ramp during the active phase of the modulation signal.
3. The voltage ramp drives the voltage-controlled oscillator (VCO) which outputs a linear frequency modulated signal referred to as a chirp. The chirp bandwidth is at 375 MHz centered at 94 GHz and the chirp rate is at 3 MHz/usec.
4. The chirp signal is amplified and divided into 2 identical signals. One version of the signal is fed to one of the transmit antennas and emitted into the atmosphere. The other version of the chirp is input to the de-chirp mixer (discussed below).
5. A portion of the transmitted energy reflects off objects in the radar's FOV and is intercepted by the receive antenna.
6. The received energy is amplified and input to the de-chirp mixer. The de-chirp mixer subtracts the frequency of the received signal from that of the transmitted signal. Therefore, the de-chirp mixer output signal frequency is proportional to the range of the object which reflected the energy. (This is a fundamental concept of FMCW radar.)
7. The de-chirped signal is fed to the Automatic Gain Control (AGC) amplifier which adjusts the signal level to keep it within the dynamic range of the analog-to-digital (A/D) converter. The AGC control signal is generated by the sensor control circuitry located in the DSP Module.

8. The IF signal is further amplified and low-pass filtered before the A/D converter digitizes the de-chirped signal so it can be processed by the FLAR's DSP circuitry.
9. The DSP circuitry uses frequency-domain analysis to determine range to deteeted objects and sequential range differentiation to determine relative range rate.

The radar pulse has a signal bandwidth of 375 MHz centered at 94 GHz. The received signal is de-chirped and down-converted to a base band signal with a bandwidth of 2 MHz.

The description above corresponds to the sequence involved in processing a single radar pulse. The TRW FLAR integrates the energy from multiple pulses to improve the signal-to-noise ratio and therefore increases the sensor's detection capability. Depending on the mode, the TRW DSP electronics will integrate the returns from five or six pulses.

The ERIM interface with the radar IF signal occurs prior to any digitization, as illustrated in Figure 4-l. Therefore, the ERIM data collection system A/D converter has an input signal similar to that of the TRW DSP Module (see Appendix C). ERIM's processing algorithms can analyze both individual and groups of pulses.

4.3.2 Timing Specifications

As mentioned above, the FLAR processor integrates a number of pulses together to improve the signal-to-noise performance of the radar. Each group of pulses is fully processed and an update provided over the RS232 interface before the next group of pulses is transmitted. A radar frame consists of one set of pulses and the processing time before the next set of pulses is transmitted-this also corresponds to the data update rate of the sensor. The rate at which pulses are sent out is known as the pulse repetition frequency (PRF). The number of pulses within a group is dependent on the operating mode. The sensor timing parameters for the FLAR are shown in Table 4- 1.

Table 4-l FLAR Timing Parameters

Parameter	Value	Description
Pulse Duration	123 mS	Length of each transmitted pulse
Pulses/Group	6	Acquisition Mode
	6	Tracking Mode
	5	Surveillance Mode
Pulse-pulse Time	1.87 mS	Equivalent PRF of 535 Hz
Frame Time/Update Period	50.2 mS	Equivalent Frame PRF 20 Hz

The timing diagram in Figure 4-2 illustrates the radar timing parameters for the tracking and acquisition modes. The tests conducted during this program used only the acquisition and tracking modes of the FLAR and, therefore, always had 6 pulses per radar frame.

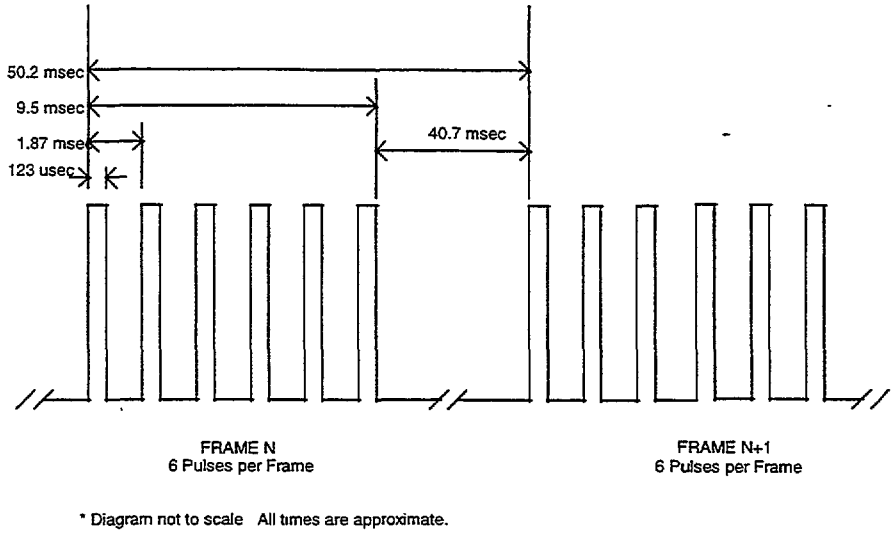

Figure 4-2. FLAR Transmit Pulse Timing

4.3.3 Automatic Gain Control (AGC) Amplifier

As described earlier, the FLAR's automatic gain control (AGC) amplifier keeps radar return levels within the dynamic range of the A/D converter. The plot below illustrates the attenuation (reference to maximum amplifier gain) of the AGC amplifier. The x-axis corresponds to the control voltage applied to the AGC amplifier and the y-axis is the corresponding attenuation in dB.

It was critical that the ERIM collection system monitor the AGC control voltage being sent from the DSP module to the RF head, so that the analysis procedures could account for effects of the AGC on the signal return levels observed during the tests.

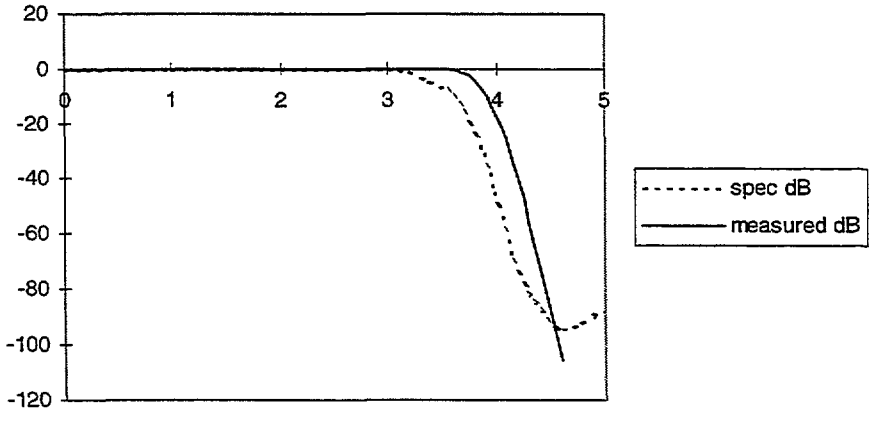

Figure 4-3. AGC Attenuation (dB) Versus Voltage (Volts)

4.3.4 Transmitted Waveform

The FLAR generates a linear FM signal referred to as a chirp. Both time and frequency domain representations of a chirp signal are provided in Figure 4-4.

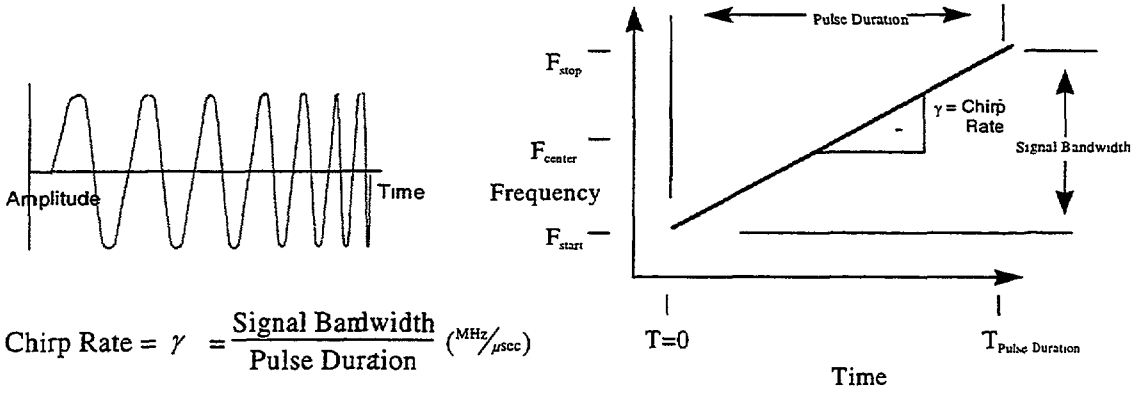

Figure 4-4. Graphical Representations of a Chirp Waveform

This form of signal is typical in FMCW-type radars. It is the frequency modulation of the transmitted signal which allows the range-to-targets within the sensor's field-of-view to be calculated. As shown in Figure 4-5, using a chirp signal results in the range being proportional to frequency.

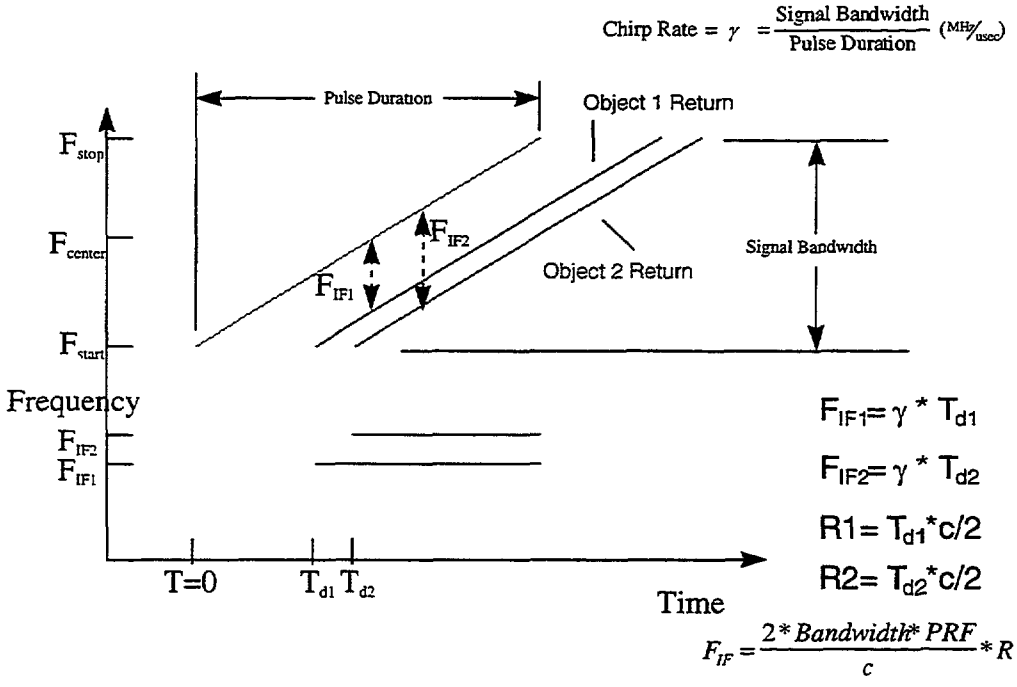

Figure 4-5. Range in Proportion to IF Frequency

The frequency which a remote sensor uses (e.g., 77 GHz or 94 GHz) determines how the energy interacts with objects in the environment. For example, lower frequency emissions tend to penetrate materials more than higher frequencies. The bandwidth of the transmit signal determines the range resolution for FMCW sensors such as the TRW FLAR.

For the purposes of this program, measuring the transmit waveform parameters served to verify both FLAR stability and the frequency and bandwidth specifications reported by TRW. Also, the bandwidth value was used in conjunction with the transmit time (discussed in the previous section) to determine the chirp rate. The chirp rate allowed the frequency domain analysis of the return signals to be correlated

with the actual range to objects in the sensor field-of-view. The transmit waveform parameters are summarized in Table 4-2.

Table 4-2. Transmit Waveform Parameters

Parameter	Value
Center Frequency	94.165 GHz
Bandwidth	375 MHz
Chirp Rate (calculated)	3.048 MHz/usec

4.3.5 Intermediate Frequency Signal

The TRW FLAR intermediate frequency (IF) waveform parameters correspond to the signal which is input to the sensor receiver A/D converter. The IF signal was considered the raw FLAR sensor output and all the digital signal processing was performed on this signal. The parameters of concern for the IF signal are frequency, bandwidth, and voltage level. These parameters dictated the required specifications of the A/D converter and any signal conditioning (e.g., amplification) required prior to the A/D. The FLAR IF signal parameters are summarized in Table 4-3.

Table 4-3. IF Signal Parameters

Parameter	Value
Frequency	DC to 2 MHz
Bandwidth	2 MHz
Voltage Range	-1 volt to + 1 volt

4.3.6 Power Measurements

The transmit power level of a radar affects the signal-to-noise ratio of the return echoes in the sensor's receiver. The higher the transmitted power, the stronger the return echoes from objects in the scene. Therefore, from a signal-to-noise perspective, the higher the transmit power the better. However, implementation, cost, and safety issues limit the transmit power level.

The results of direct measurements of the FLAR transmitted waveform are given below:

- Left Beam: 21.7 mW
- Center Beam: 26.6 mW
- Bight Beam: 22.3 mW

These values correlate with the antenna beam pattern measurements made on ERIM's rotary platform. Figure 4-6 indicates that the left and right transmit beam power emissions are down slightly from the center beam.

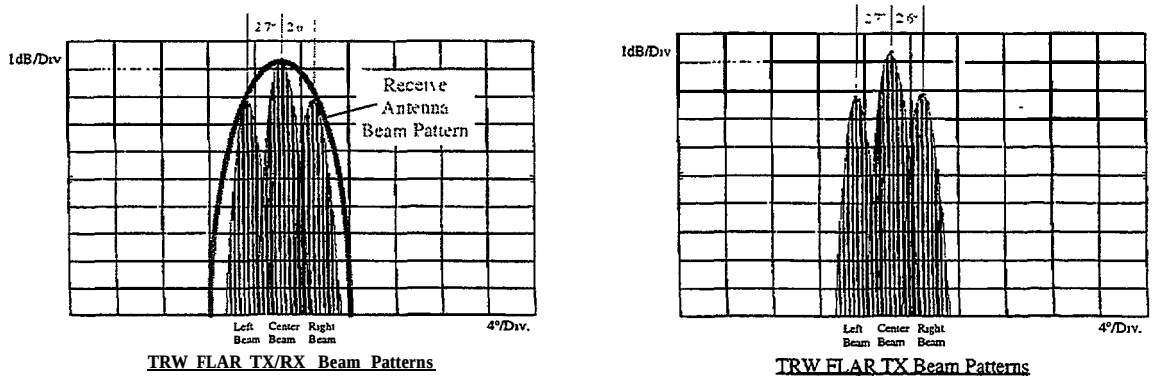

Figure 4-6. FLAR Beam Patterns

4.3.7 Antenna Beam Patterns

The FLAR sensor uses three beams pointed to the left, center, and right of the sensor boresight (i.e., the vehicle center line). Figure 4-3 illustrates the FLAR beam patterns and their orientation with respect to each other. TRW uses the three-beam approach in order to implement a search and track algorithm for an Automated Cruise Control (ACC) application.

Because the goal of this program was to view the FLAR as a generic radar sensor, the TRW beam switching algorithm was not employed in the testing. An override switch was used to manually select an active transmit beam during any particular test.

4.3.8 Beam Switch Isolation

As described earlier, the TRW FLAR uses a switch to direct the transmit signal to one of three separate antennas. The isolation between the different ports of this switch are provided in Table 4-4.

Table 4-4. Beam Switch Isolation

	Right Beam (dB)	Left Beam (dB)	Center Beam (dB)
Left Beam	18.7	I 0	16.2
Center Beam	34.3	30.3	0
Right Beam	0	15.9	18.6

4.4 BASELINE PERFORMANCE CHARACTERISTICS

4.4.1 Radar Field-of-View

The radar's field-of-view is directly related to the antenna beam patterns discussed above. Several tests were conducted to determine the basic field of view of the sensor (see Appendix A). These tests found, as expected, good correlation between the measured beam patterns and azimuthal detection of targets.

Typically, antenna beam widths are specified in terms of their 3 dB points, which correspond to locations in the beam pattern where the antenna gain is down 3 dB from its maximum gain. In the case of the FLAR, each transmit beam has a 3 dB width of 3 degrees in both azimuth and elevation. This

corresponds to a beam width of approximately one lane width, at 80 meters from the radar. However, as illustrated in Figure 4-7, the antenna patterns can detect objects well outside their 3 dB points.

The results of measurements taken on ERIM's rotary platform measurements are shown in Figure 4-7. These plots show the mainlobes along with the sidelobes for the center, right, and left antenna beams respectively. A "zoomed" in version on the mainlobes for each antenna was provided in Figure 4-6.

The left and right antenna beams show a sidelobe about 12-15 dB below the mainlobe. The left beam sidelobe is approximately 4.5 degrees from the left beam mainlobe. The right beam sidelobe is approximately 6.5 degrees from the right beam mainlobe. The 3 dB beam width on all three beams is approximately 2.7 degrees wide.

Knowledge of these beam patterns is essential in evaluating the performance of the FLAR during roadway testing. Antenna sidelobe levels can significantly affect the performance of the sensor. For example, a 30 dBsm target azimuthally located within the sidelobe of the left beam would be interpreted by the sensor as a 15 to 18 dBsm target located in the mainlobe of the left antenna.

Taking this issue a step further, a large target located outside the 3 dB point of the center beam (i.e., outside the road lane) could appear to be a somewhat smaller target located inside the road lane.

Several of the roadway tests in this program are designed to address these issues. Using the typical 3 dB point specification, the 3-antenna approach provides the FLAR with an approximately 8.3 degree azimuth field of view.

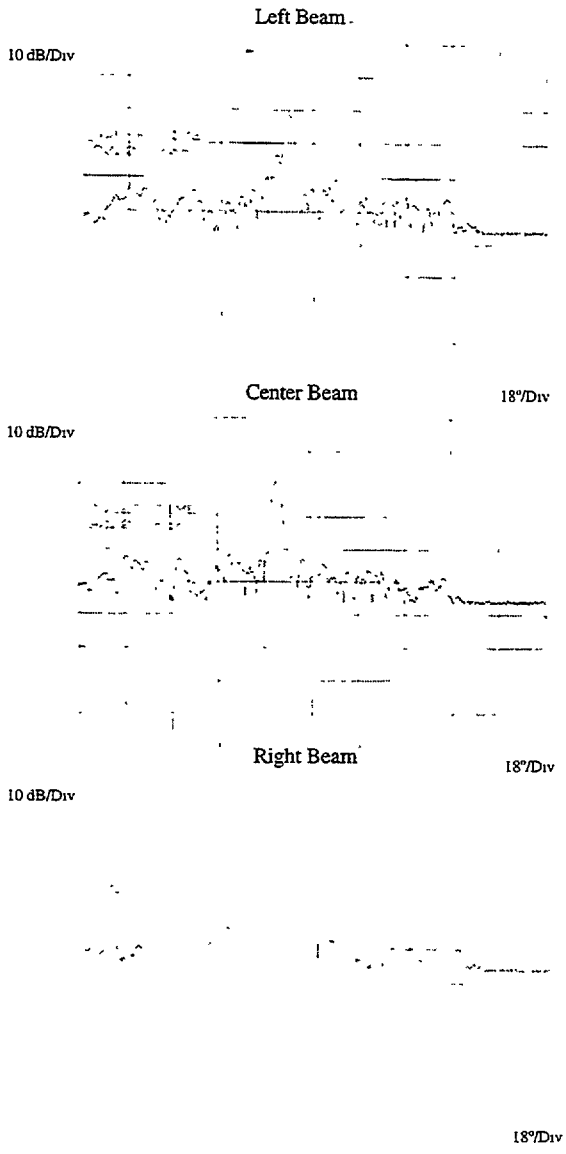

Figure 4-7. FLAR Beam Patterns

4.4.2 Range Accuracy

The range tests are a set of static tests designed to measure the absolute accuracy of the FLAR sensor. Targets were placed at known distances and data was collected for analysis using ERIM-developed processing software (in other words, only the raw radar signal was being considered, to avoid evaluating TRW's particular processing algorithms). The tests were divided into two distinct sets: (1) Far Range Tests and (2) Near Range Tests. This section will discuss the results from both sets and relate the findings to expectations for other automotive radars.

4.4.2.1 Far Range Tests (10 to 100 meters)

Data for these tests was collected by placing a corner reflector at 10 meter increments from 10 to 100 meters from the FLAR sensor. Individual tests were run using a 10 dBsm and 20 dBsm target to evaluate correlation between the results.

Figure 4-8 shows the results for the 20 dBsm and 10 dBsm corner reflectors. The solid line represents the mean detected distance and the dotted lines show one standard deviation from the mean. The dot-dashed line shows the distance reported by the FLAR sensor (which utilizes the TRW processing algorithms).

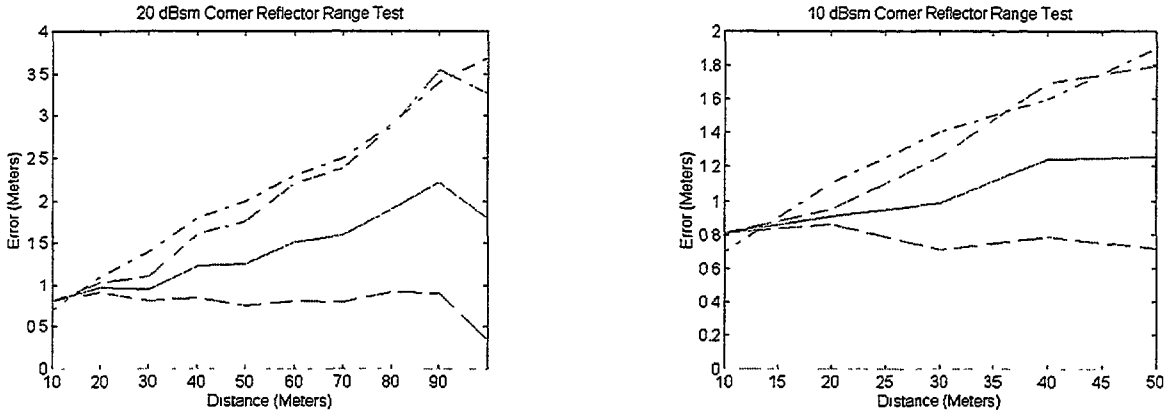

Figure 4-8. Corner Reflector Range Test Results

The figures show both a nonzero slope and a DC offset. The DC offset is an unaccounted for static error in the either the FLAR sensor or the test setup/analysis routine. The slope is due to a chirp rate discrepancy. That is, the chirp rate is not really what the specification says it is. Figure 4-9 shows how a discrepancy in the chirp rate can lead to an error in the reported target range. The vertical lines (Actual/Theoretical Dechirped Frequency) correspond to the sine wave created when the sensor dechirps the return from the target. The frequency of the dechirped sine wave is:

$$f = \frac{d\gamma}{c}$$

where f is the frequency of the dechirped sine wave

d is the distance from the sensor in meters

γ is the FLAR sensor chirp rate in MHz/μs

c is the speed of light in meters/μs

For a given chirp rate there is a unique frequency, for every range. However, if the chirp rate changes, then the one-to-one correspondence between range and frequency also changes.

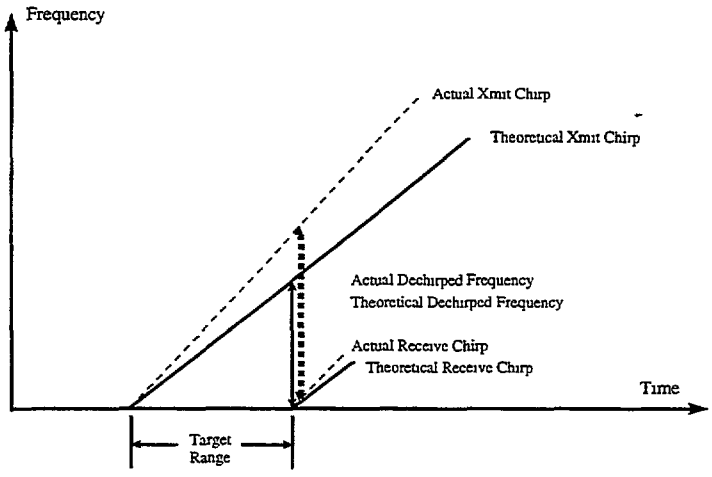

Figure 4-9. Effect of Chirp Rate Error

Using the actual measurements taken in these tests, a true chirp rate was calculated using information from Figure 4-8 as follows. The actual method used was to fit a line to the mean value data on Figure 4-8 and use information from that line to calculate the new values.

Let

$$d_1 = \frac{fc}{\gamma}$$

$$d_2 = \frac{fc}{\gamma + \Delta\gamma}$$

where d_1 is the assumed distance using the TRW numbers

d_2 is the measured distance (from Figure 4-10)

f is the frequency of the dechirped sine wave

c is the speed of light

γ is the chirp rate

$\Delta\gamma$ is the unknown difference in chirp rate to be calculated

The figure shows the error term obtained by subtracting d_1 from d_2. That is, the theoretical chirp rate value was used to calculate the distance given the sine wave data. Therefore the range dependent error (known because the actual distance was measured during the experiment) was caused by using the wrong chirp rate. In equation form the distance error is:

$$\Delta d = d_2 - d_1 = \frac{fc}{\gamma} - \frac{fc}{\gamma + \Delta\gamma}$$

Solving this equation for $\Delta\gamma$ gives the following:

$$\Delta\gamma = \frac{-\gamma^2}{\gamma - \frac{fc}{\Delta d}}$$

where $\gamma = 3.04878$ MHz/μS

$c = 300$ m/μS

f is chosen arbitrarily

Δd is chosen from the best fit line derived from Figure 4-9, given f

Adding in this correction to the chirp rate results in a range error profile that is nearly flat. However there is still a static offset that has to be removed. This was accomplished by noting the y intercept point from the line fit procedure during the chirp calculations. Applying both corrections and re-running the Matlab analysis software yielded the results shown in Figure 4-10. As expected the error was zero mean with a standard deviation proportional to range. The same correction coefficients were then applied to the results from the 10 dBsm corner reflectors; if the error was an effect of the sensor then correction coefficients should work for all test setups. The new chirp rate and offset values were:

$\gamma_{new} = 3.09319$ MHz/μs (Compared to 3.04878 theoretical)

Static Offset = 0.633727 Meters

The results of using these new correction values in the data processing is shown in Figure 4-10 for the 20 dBsm and 10 dBsm reflectors. As expected the range errors now had a zero mean with a standard deviation proportional to range. Since the error was attributed to a chirp rate discrepancy, the corrections were expected to work for all test set-ups. In fact, this proved to be the case, as a comparison of the first 50 meters of the 20 dBsm range test was almost identical to the 10 dBsm range tests. (Note that the 10 dBsm target was not detectable beyond the 50 meter mark.) **Therefore, the new chirp rate parameter and offset were be used throughout the program.**

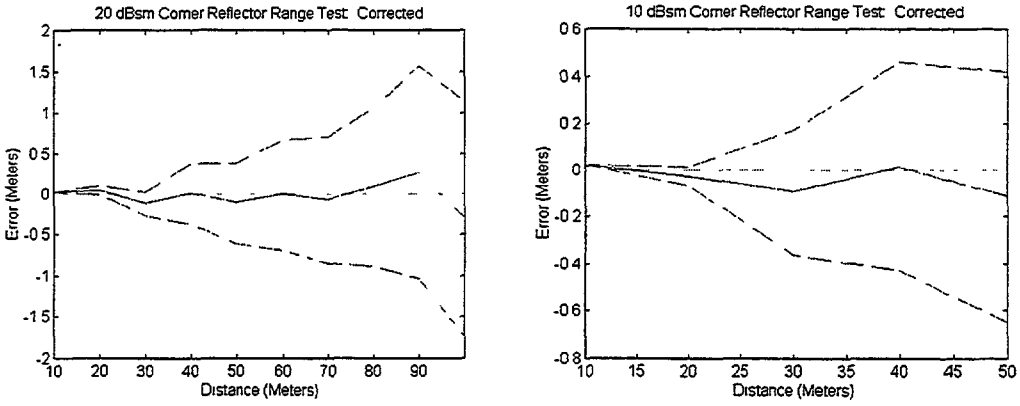

Figure 4-10. Corrected Corner Reflector Range Test Results

In summary, the FLAR sensor showed both a static offset and a range dependent error. These errors can be corrected by calibrating the sensor using radar range measurements to calculate two correction coefficients. In addition, the sensor shows an increase in reported range variations as the range to the target increases. The following section on range resolution provides a detailed discussion on the effects of transmit and receive signal phase errors. These can result in a greater variation of reported target range as the actual range to the target increases.

The actual results of this test are specific to the TRW FLAR sensor. However, it is likely that the 'offset' and 'linear' errors discussed in this section will occur in other radars designed for automotive applications. The methodology for correcting these errors is a calibration process which will determine:

1. Variable signal delays through the radar components, which result in offset errors.
2. Variations (from spec) in the transmit signal FM modulation (Chirp Rate), which results in linear range errors.

The correction of values resulting from such a calibration process can be implemented in the sensor's processing algorithms and require no "fine-tuning" of the hardware. With appropriate instrumentation, this process can be substantially automated.

The magnitude of the offset and linear errors will be dependent on the quality of the components used in the system. Therefore, cost versus performance versus required calibration effort trade-offs will have to be correctly evaluated for production of automotive radar sensors. For example, a common approach to creating a linear frequency modulated signal (i.e., a chirp) is to drive a voltage-controlled oscillator (VCO) with a voltage ramp. The quality (linearity, spectral purity, etc.) of the VCO output signal is proportional to the component cost. Therefore, it is critical that automotive radar design engineers understand the overall radar system performance implications on a component by component basis.

Besides considering the absolute magnitude of the offset and linear ranging errors, the system designer must evaluate a particular system's sensitivity to such errors. This sensitivity evaluation must include the radar processing and threat assessment algorithms employed by the system. For example, a system employing range differentiation to determine range rate (as opposed to Doppler processing) will be highly sensitive to the variations in the range reported by the FLAR sensor in these tests.

4.4.2.2 Near Range Tests (0 to 10 meters)

This next set of tests was aimed at evaluating performance as targets approached the near-field antenna range. It also demonstrates the effects of a physically small target close to the FLAR's two-antenna bistatic arrangement. A bistatic arrangement refers to the fact that the FLAR uses physically separate transmit and receive antennas (some radars use a duplexor to allow a single antenna to function for both transmit and receive).

The issue of near-field versus far-field radar measurements was discussed in Section 3 with regard to the radar cross-section measurements. For these near-range tests, the near-field issues must be considered. In the near field the antenna beam pattern can be assumed to be the same shape as the antenna aperture. The space around an antenna is divided into three regions, the reactive near-field region, the radiating near-field region, and the radiating far-field region. The boundaries between these regions are dependent on the antenna design. However certain criteria are generally used to denote the boundaries between the regions. The reactive near-field region ends at a distance $\lambda/2\pi$ from the antenna, where λ is the transmitted wavelength. The commonly used definition for the boundary between the near-field and far-field regions is:

$$R = \frac{2D^2}{\lambda}$$

where R is the boundary distance from the antenna

D is the largest aperture dimension

λ is the transmitted wavelength

For the FLAR antenna the reactive near-field region is approximately 0.5 mm. This battery of tests never operated in that region. The radiating near-field region extends out to approximately 3 meters.

The FLAR collection system was set up in the ERIM highbay facility. A piece of radar absorbing material was placed between the sensor and the far wall in order to eliminate undesired returns. A 10 dBsm corner reflector was placed in front of the sensor at a range of 10 meters and a set of radar pulses was collected. The reflector was moved one meter closer, and the process was repeated, until the reflector was 1 meter from the sensor. The range data was analyzed using the same analysis routines described the previous section.

Processing of the various data sets resulted in the plots shown in Figure 4-11. The solid line represents the mean detected distance and the dotted lines show one standard deviation from the mean. The dot-dashed line shows the distance reported by the FLAR sensor (which utilizes the TRW processing algorithms). Note that the static offset and chirp rate corrections determined in the far range tests (see discussion above) were employed while processing the near-range data sets.

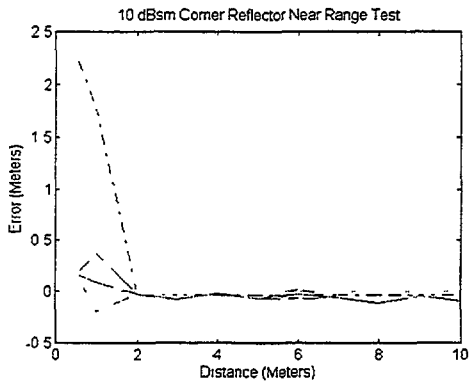

Figure 4-11. 10 dBsm

Figure 4-12. 10 dBsm at 1 Meter

The plot indicates that the FLAR accurately measured the target's range until the target was placed closer than 2 meters. The measurement taken at 1 meter shows a significant error in the ERIM processed data (i.e., the raw radar signal); the error is extreme for the TRW processed data.

A single return pulse for the 1 meter distance is shown in Figure 4-12. The figure shows two distinct peaks, one at the target distance and one at roughly twice the distance. The FLAR sensor reported the ghost target (at the further distance) as the real target and ignored the real target. The data shows that the target was detected at the appropriate range. The FLAR sensor software for some reason chooses to detect only the ghost target.

Figure 4-13 shows a plot of 100 consecutive pulses from the FLAR sensor. The second "ghost" target is always present. The second target is caused by one of three effects. First, it could be caused by too much power reflecting back to the FLAR sensor. This could make the RF front end saturate, causing the circuit to operate in the nonlinear region. Second, it could be caused by energy reflecting back into the transmitter, which would also cause the circuits to act in an unpredictable fashion. Third, the target may be an effect of multipath reflections. This would be a case where the radar bounces off the target, then the vehicle, then the target again.

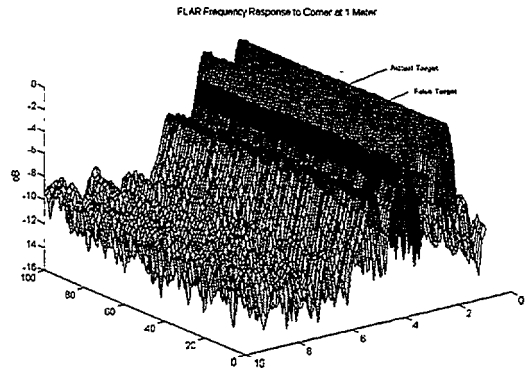

Figure 4-13. FLAR Frequency Response to Comer at 1 Meter

Due to ERIM's limited access to the TRW hardware and processing algorithms, the cause of the double peaks in the radar data could not be experimentally determined.

In summary, the FLAR sensor does not operate reliably at ranges less than 1 meter. The error can cause a target to appear farther away than it really is. This could have disastrous consequences in real world intelligent cruise control or collision avoidance situations.

4.4.3 Range Resolution

The ability to separate signal returns into reflections from distinct targets or objects is described by a radar's range resolution specification. The TRW FLAR has a stated range resolution of 0.5 meters.

The theoretical range resolution of a chirped radar system is given by the following equation:

$$Pr = \frac{C}{2B}$$

where pr is the range resolution in meters

C is the speed of light: $3 * 10^8$ m/s

B is the processed bandwidth

The theoretical resolution of the FLAR system, using the documented bandwidth of 375 MHz, is 0.4 meters.

A typical way of measuring the resolution of a radar system is to measure the IPR 3 dB beam width from a point target. This can be accomplished by using any of the range data collected for the range accuracy tests. The effect of limited resolution is seen as a combining of the peak responses from two physically close targets. This effect can be seen in Figure 4-14.

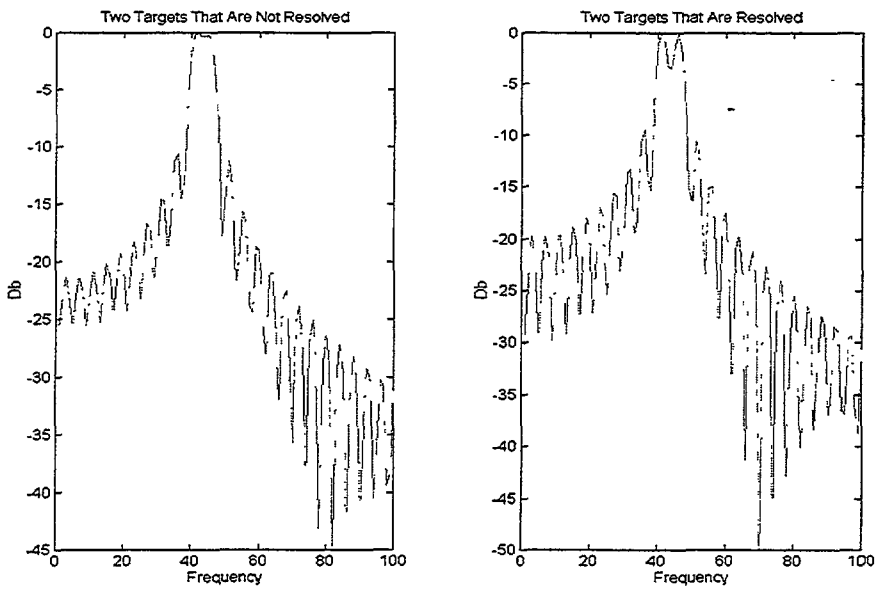

Figure 4-14. Effect of Limited Resolution

The resolution of the sensor system is degraded by nonlinearities in the transmitted chirp signal. If these errors are static pulse-to-pulse then they can be removed either by predistorting the waveform (an expensive alternative) or by post processing of the collected data. If the errors are not the same pulse-to-pulse, the system performance can be only marginally improved by post processing. Correction requires modification of the waveform generation circuit to remove the pulse-to-pulse instabilities.

Two approaches were used to characterize the FLAR range resolution. First was an analytical approach to determine the IPR width of the FLAR's dechirped signal; the second was a physical experiment using two displaced corner reflectors located within the FLAR's field of view.

Analytical Approach

Since the system uses a dechirped approach, only the difference of the phase error between the two chirps is available for study. This is shown in the following discussion.

The phase of a single transmitted chirp is given by:

$$\phi_T(t) = 2\pi\gamma t^2 + 2\pi f_0 t + \phi_E(t)$$

where γ is the chirp rate in MHz/microsecond,

f_0 is the initial starting frequency, and

$\phi_E(t)$ is the unknown phase error on the chirp waveform

(t) denotes a function of time (in microseconds).

Some time later the same signal is received from a target in the scene. The received signal will be a duplicate of the transmitted one, delayed by a time equal to the two-way propagation delay to the target. This assumes a non-moving target and non-moving sensor. The receive phase is given by:

$$\phi_R = 2\pi\gamma[t-\tau_D]^2 + 2\pi f_0[t-\tau_D] + \phi_E(t-\tau_D)$$

where τ_D is the time delay (two-way) from the target, and

[t] denotes straight multiplication.

After dechirping the phase of the receive signal is:

$$\phi_\Delta = 4\pi\gamma t\tau_D - [2\pi f_0 - 2\pi\gamma]\tau_D + \phi_E(t) - \phi_E(t-\tau_D)$$

The first term is the linear phase component of the received sine wave. The second term is a phase delay equal to the round-trip time to the target. The final two terms make up the difference of the phase error.

The plots in Figures 4-15 summarize the analytical results. The figure shows that the 3 dB width of the IPR for a 10 dBsm target located 10 meters from the radar is very close to the theoretical value and within TRW's stated specification. However, there is a substantial degradation in performance for a the same target located 40 meters from the radar.

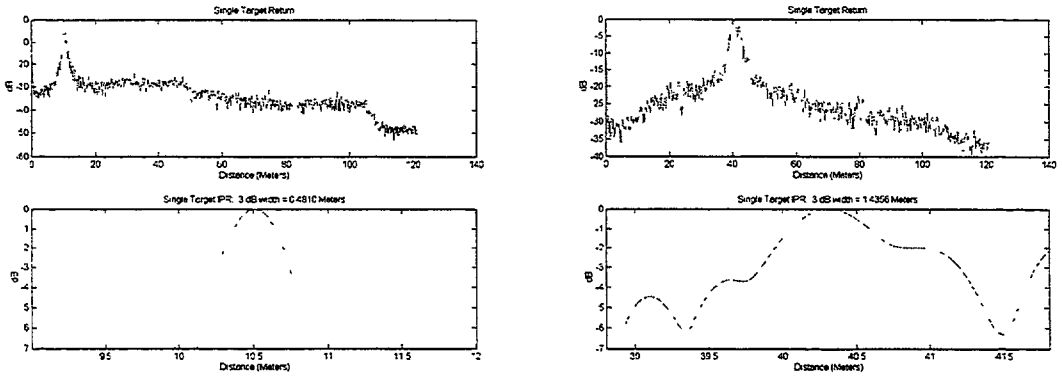

Target at 10 meters

Target at 40 meters

Figure 4-15. Performance With a Single 10 dBsm Target

As the target moves away from the sensor, the main beam starts to broaden as it is corrupted by nonlinearities in the FLAR. The performance degradation is similar to a synthetic aperture radar (SAR) problem ERIM encountered in the early 1980's and is caused by phase errors in the transmitted chirp. At near ranges the errors are small, but as the range increases the error becomes more noticeable.

In the case of the FLAR sensor, the phase errors causing the degraded IPR response were found to be of two different types. First, there is a quadratic phase error caused in part by waveguide dispersion. That is, the waveguide does not have constant phase characteristics over the bandwidth of the transmitted chirp. It could also be caused, in part, by other circuits with nonlinear phase characteristics. However there was no access to the circuit during this test so it is impossible to determine exactly where the error is being introduced.

The quadratic error causes a broadening of the mainlobe of the IPR, which decreases the system resolution. However, it does not explain the mainlobe corruption in Figure 4-18. The corruption resembles a sinusoidal phase error of many cycles per transmit pulse. A thorough signal analysis indicates that the transmitted signal is being distorted by a roughly 40 KHz sinewave within the radar.

A test sine wave was created and a sinusoidal phase error of 40 KHz was added to demonstrate the effects of sinusoidal phase error on a pure tone. The results, along with an actual FLAR sensor return, are shown in Figure 4-16. The middle plot of Figure 4-16 and the right plot are very similar in that they

have a mainlobe with very high sidelobe levels. Also of note is the asymmetry around the mainlobe. Both plots show a similar asymmetry, with the right side (far range) falling off faster than the left side (near range).

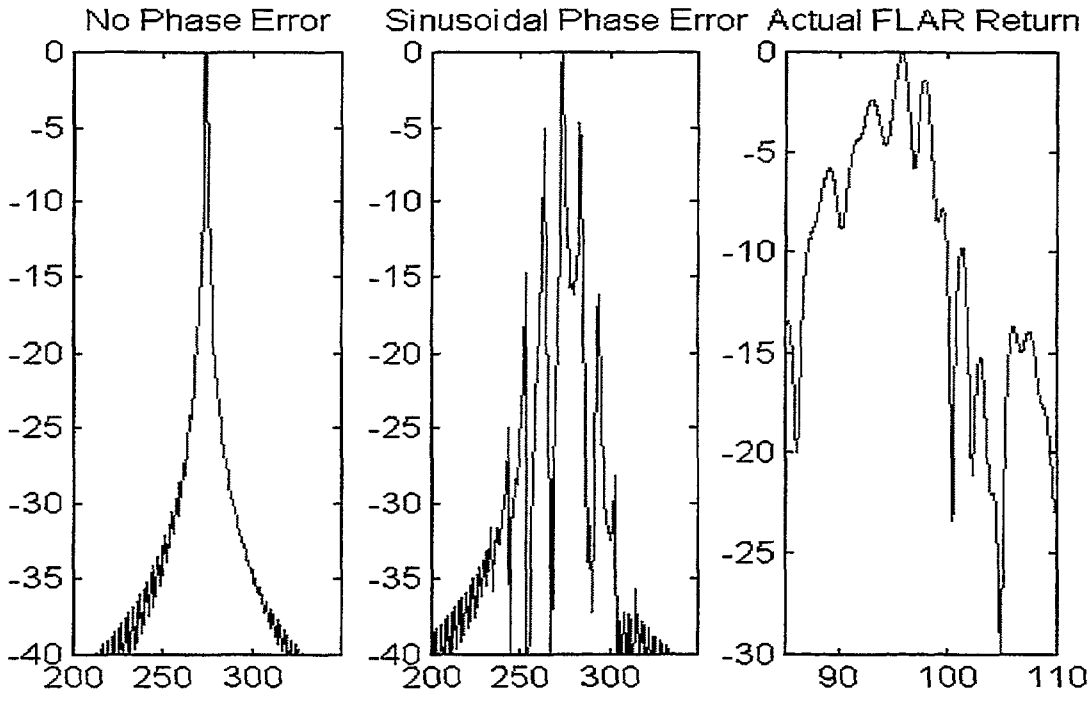

Figure 4-16. Effects of Sinusoidal Phase Error

Sinusoidal phase errors are worse at far ranges than they are at near ranges. This is because the dechirping process shows the phase errors as the difference between the transmitted and received error. Two sine waves with little phase difference (i.e., a small time delay with respect to their period) subtract leaving a small residual. As the phase difference increases the difference becomes larger. When the errors are out of phase the difference can actually be larger than the original phase error (constructive interference).

It is this sinusoidal error within the FLAR transmit chirp which causes the range accuracy deviations identified in the range accuracy tests discussed above.

With this analytical knowledge, the physical tests of FLAR range resolution performance were performed at near ranges to avoid the errors induced by the sinusoidal distortion.

Empirical Approach

This test used data previously collected for the range accuracy tests. However, the analysis differed. Only one set of six pulses was used. This data was heavily up-sampled by zero padding the FFT to 32768 (32K) points. This allowed an accurate measurement of the 3 dB IPR width.

A resolution demo was performed in the ERIM highbay facility using two similar corner reflectors placed close together. The corners were placed approximately 5 meters from the FLAR sensor. The corners were mounted on a low reflectance (cardboard) flat plate marked off in 0.1 meter increments. The flat plate was mounted on a 0.7112 meter (28 inch) high Styrofoam pillar. The corners were

initially set at a distance of 0.6 meters and moved in a tenth of a meter every collection thereafter. The comer reflectors were nominally sized to be 11.6 dBsm.

In these tests, the sensor was able to reliably resolve two similar sized objects placed more than 0.6 meters apart. At relative distances less than 0.6 meters, the sensor would sometimes resolve them and sometimes not. This matches fairly well with the theoretical analysis discussed above.

With regard to a generic automotive radar, the range resolution is important, as it allows the system to track and identify multiple objects. As shown, the quality of the transmit signal plays a major role in the range resolution performance of the radar. This of course relates back to the cost-performance trade-off which must be made by system developers in implementing a specific radar sensor design.

4.4.4 Baseline IF Signal Characteristics

The last baseline characteristic of interest in this program is the typical range profile produced by the FLAR when mounted on the ERIM TBV and presented with an "empty" roadway environment. The "empty" roadway environment refers to being on a typical roadway without any other vehicles or objects to produce a return.

Figures 4- 17 and 4-18 show range profile plots for 160 frames of radar data collected on an empty roadway. Figure 4-17 shows the range profile with the return levels on the y-axis and the corresponding range on the x-axis. Each profile from the 160 frames is overlayed on this plot. Figure 4-18 is a similar plot, except that instead of overlaying the profiles from each frame, a third dimension on the plot is used to position the frames side-by-side to produce a "time-history" of the returns. Both of these plots were made from the same set of data.

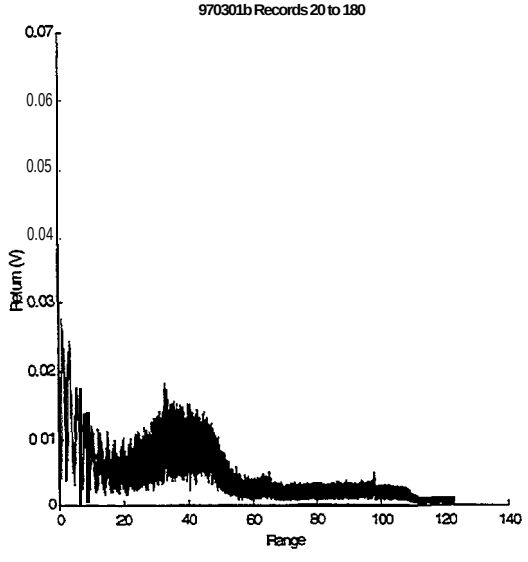

Figure 4-20. Two-Dimensional Range Profile Plot

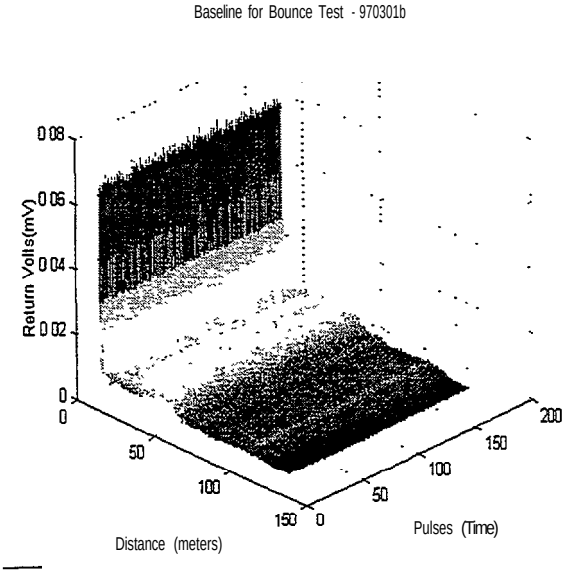

Figure 4-21. Three-Dimensional "Time History" Range Profile Plot

The FLAR exhibits a clear range profile characteristic which has been observed throughout the evaluation of the unit. First is the very-near-range return which is significantly above the noise floor of the sensor. This near-range return is attributed to leak-through of the transmit signal into the receiver circuitry. While this "return" is well above the noise floor, it does not compete with the return levels from any significantly sized objects. The TRW processing algorithm does not recognize this return as a target.

The second characteristic is the "'hump" which appears at ranges between approximately 30 to 45 meters. Initially, this hump was attributed to the range at which the antenna beam pattern intersected with the roadway surface. However, "bounce tests" were found to have no effect on the characteristic hump. Therefore, this hump is attributed to some distortion or response within the FLAR receiver circuitry.

These baseline characteristics of the FUR IF signal were considered in the analysis of data collected on the natural roadway.

5.0 MATERIALS AND THE ENVIRONMENT

This section will present the results of testing designed to quantify the effects of various materials and environmental conditions on FLAR performance. In these tests, the FLAR was being treated as a "generic" 94 GHz radar sensor. That is to say that none of the TRW algorithms associated with the ACC application were employed in arriving at these results.

The tests were conducted by carefully controlling the environment presented to the radar sensor and recording the raw radar signals, to evaluate changes based on the environmental conditions. The tests are divided into three sections: (1) Materials Testing, (2) Precipitation Testing, and (3) Contamination Testing. The results are summarized below and described more completely in Appendix B.

5.1 MATERIALS TESTING

The materials testing experiments were designed to quantify the amount of attenuation experienced by the radar signal when it is transmitted through various types of materials. This testing indicates the types of materials which should be considered for the housing of an automotive radar. The testing also identifies materials which the radar may have a difficult time detecting on the roadway.

The types of materials tested were:

- Plexiglas
- Windshield-type Glass
- Epoxy Glass
- Thin Cardboard
- TPO (a flexible plastic commonly used in automobile bumpers/facia)
- 3/4" Plywood
- RAM (Radar Absorbing Material)

The testing procedure consisted of placing a 5dBsm comer reflector at approximately 20 meters from the FLAR. Data was then collected as a sample of each material was placed between the FLAR and the comer reflector. Appendix B provides a complete description of the testing procedures and analysis. Also included in Appendix B is a brief explanation of the mechanisms which cause conductive and non-conductive materials to reflect energy.

5.1.1 Results

Three effects were observed during the material obstruction tests: (1) target signal strength attenuation, (2) direct reflection from the material being tested, and (3) creation of multipath returns. Each of these effects are discussed below.

Attenuation

Table 5- 1 summarizes the attenuation results of the material tests. The return levels and AGC settings for each collection are provided. These measured parameters were used to calculate the "AGC adjusted voltage" values which were then compared to determine the attenuation levels. The "Baseline" measurement was used as the reference for each attenuation calculation. Note that the attenuation levels provided are for "two-way" propagation. In other words, the radar signal passed through the material under test twice---once on transmission, and once after it was reflected off the target in the scene.

Table 5-1. Attenuation

Material Description	Measured Return Volts	AGC Control Setting (v)	AGC Mag. Attenuation (dB)	AGC Adjusted Return Volts	Two-Way Power Attenuation (dB)
Baseline	0.458	4.154	-19.9034	1.4403	0.0
Clear Plexiglas	0.405	3.956	-5.9292	0.5698	8.1
Thin Cardboard	0.4	3.906	-3.6324	0.4930	9.3
Windshield Glass (15 degrees)	0.381	3.906	-3.6324	0.4696	9.7
Epoxy Glass	0.343	3.906	-3.6324	0.4228	10.6
Thick Cardboard (corrugated)	0.188	3.906	-3.6324	0.2317	15.9
TPO	0.17	3.906	-3.6324	0.2095	16.7
TPO (15 degrees)	0.163	3.906	-3.6324	0.2009	17.1
Plywood (0.75")	0.056	3.906	-3.6324	0.0690	26.4
RAM	0.05	3.906	-3.6324	0.0616	27.4

Figure 5-1 illustrates the relative attenuation levels listed in Table 5-1. The materials are listed from lowest attenuation level to highest. Note that the RAM attenuation level represents the maximum attenuation level for the given test set-up (e.g., size and distance of target). Returns from the reference reflector placed in the scene were always observable in the radar data except for tests with the RAM. Even in tests with the plywood as the obstructing material, the FLAR still detected the 5 dBsm reference target at 20 meters.

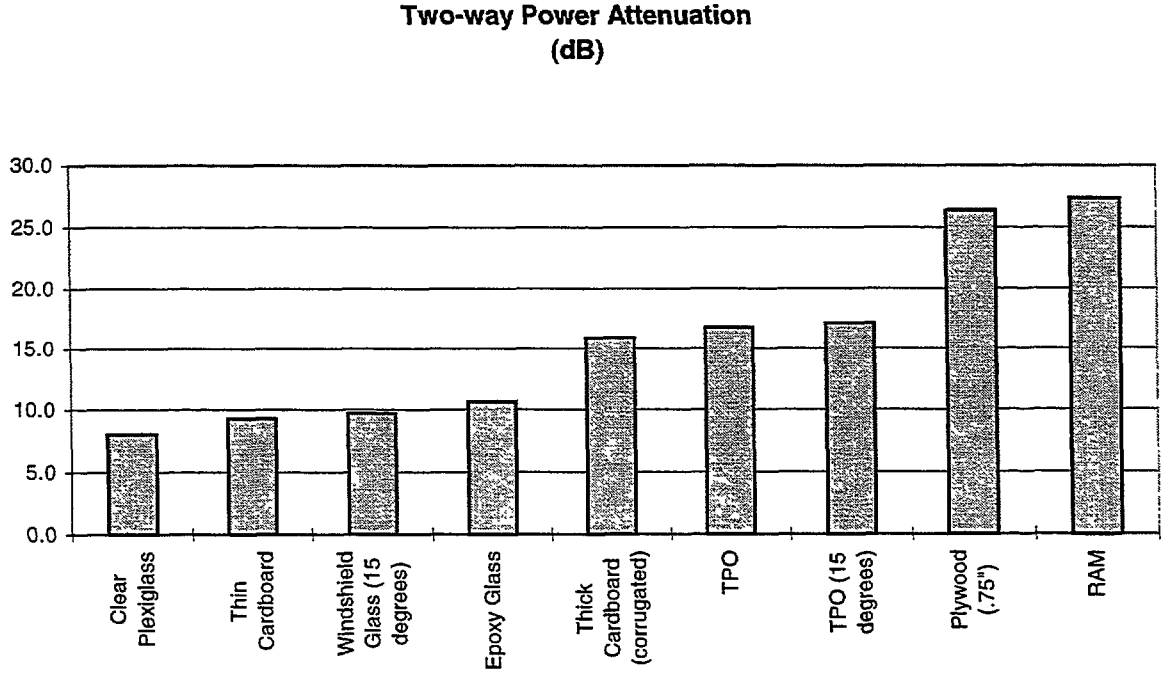

Figure 5-1. Attenuation Levels

The two-way attenuation levels vary from 8.1 dB for the clear Plexiglas to over 17 dB for the TPO (a plastic-type material commonly used for bumpers and facia styling) and over 26 dB for the plywood.

Reflections

In addition to attenuating the return levels from the reference reflector, many of the materials produced a direct radar signal return (i.e., the material reflected the radar energy). The materials producing the largest reflections were the windshield glass and TPO materials. Note that these reflection levels were highly dependent upon the orientation between the FLAR and the material sample. The plots included in Appendix B indicate that these reflection levels can be nearly equal to the return level from the reference reflector. Of course the material samples were at a much closer range than the reference reflector-l to 2 meters for the material samples versus 20 meters for the reference reflector.

Much lower direct reflections were observed from the cardboard, Plexiglas and plywood materials. While these reflections were clearly evident, they were not much above the noise floor of the FLAR.

Multipath

In addition to the reflections and signal attenuation, several of the material samples were observed to produce multipath returns from the reference reflector. Figure 5-2 is a diagram showing how an obstructing material can cause a multipath return. Some level of energy is refracted by the material and directed along an indirect path to the target. Since the distance the radar signal must travel the indirect path is longer than that along the direct path, the resulting range reading from the radar will be greater than the actual direct range to the target.

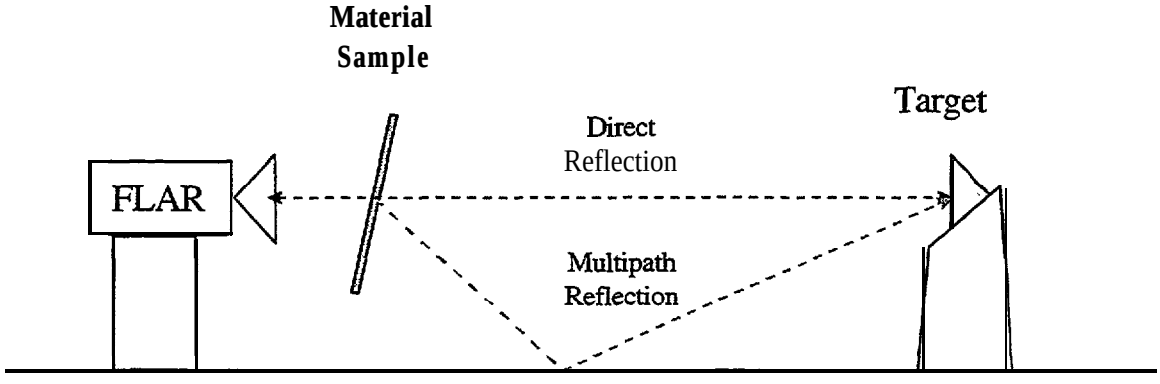

Figure 5-2. Multipath Reflection

Figure 5-3 shows the radar returns collected with a TPO material sample oriented 15 degrees off vertical. The multipath returns from the reference reflector are clearly evident. These effects were also observed for other materials tested. The effect of this phenomenon is that the peak level return from the reference reflector is decreased and false returns are produced. See the plots in Appendix B for more multipath examples.

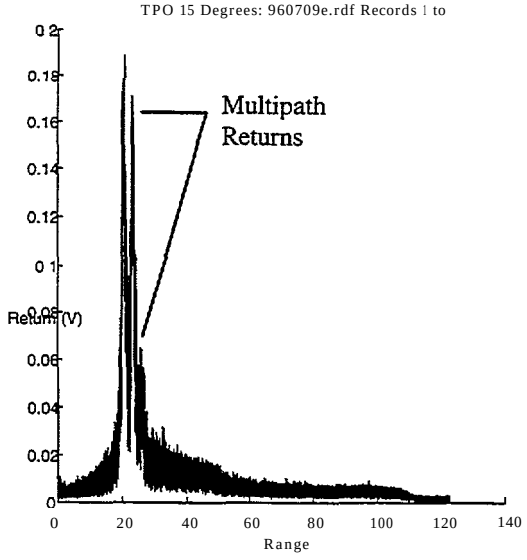

Figure 5-3. Multipath Returns From TPO Material at 15 Degree incident Angle

5.1.2 Conclusions

The tests discussed in this section have evaluated the effects of various materials on the target return levels for a 94 GHz radar. Figure 5-l summarizes the test results. The power attenuation level is provided for each material tested. Again, these attenuation levels correspond to the effects on a 94 GHz radar, but similar results can be expected at 77 GHz. Key observations of the test include:

- All materials tested allowed some portion of the radar signal to pass through the material and attenuated the radar signal to some degree.
- Except for the RAM material, the return from the reference reflector was still observable.
- Some materials reflected observable energy at certain orientations.
- Some materials produced multipath returns at certain orientations.

For styling, automotive radars will have to be integrated into the overall vehicle structure. This means the radar antennas will most likely be covered by some type of material. Knowledge of the absorption, transmitivity, and reflection characteristics of various materials is therefore critical to the successful implementation of automotive radar sensors.

These materials tests identify issues which must be addressed in order to successfully integrate a radar into the automobile. First, if the radar antennas are to be concealed by some material, the signal attenuation resulting from the chosen material must be compensated for to maintain the required radar sensitivity. Increasing the transmit power of the radar is au easy solution which may, however, have serious cost implications. Therefore, the concealing material must be carefully selected. Typically suggested locations for automotive radars would place the sensors either behind the plastic material of the front facia or grill, or behind the glass of the windshield or headlights.

The quantitative data from these tests (see Figure 5-1) indicate that placing the sensor behind a slanted windshield may produce less attenuation than placing it behind TPO-type plastic. An even better solution is to place it behind clear Plexiglas. Another option is to utilize specially fabricated material which exhibits very low attenuation; however, this could add cost to the system implementation.

In orienting the radar with respect to a concealing material, care must be taken not to produce a significant direct reflection which may saturate the radar receiver and “blind” it to other objects. Also,

and perhaps more serious from a threat assessment algorithm perspective, is the danger of having a concealing material generate numerous multipath returns. This could potentially place a large burden on the sensor processing electronics in terms of having to generate track files for objects which do not actually exist in the scene. Some level of multipath is inevitable, due to the complexity of the roadway environment, but inappropriately choosing and orienting a material in front of the radar sensor could severely compound the problem.

Another important issue regarding the attenuation characteristics of materials concerns accurately reporting the range to non-metal roadway targets. As vehicle manufacturers continue to reduce weights, the use of non-conductive plastic materials is expected to increase. As the results of these material tests indicate, the use of non-conductive materials can severely decrease the overall radar cross-section of the vehicle.

5.2 PRECIPITATION TESTS

The purpose of these precipitation tests was to evaluate the effects of snow, rain, and fog on the performance of the FLAR sensor. Since in automotive applications, the role of the radar would be to enhance the human's ability to perform during inclement weather, the sensor's performance capability under various weather conditions is critical to evaluate.

Both natural and simulated precipitation tests were conducted to arrive at the results discussed below. The snow data was derived from natural snow precipitation only. The fog data was collected using an artificial fog machine. The rain data was collected using both natural rain and rain from a high-pressure washer to allow the precipitation rate to be more controlled.

5.2.1 Results

In general, the precipitation tested had little effect on the FLAR's performance. In particular, the precipitation particles were not found to produce any significant returns to the FLAR and the attenuation levels were very small.

Table 5-2 shows the quantitative summary of the tests (see Appendix B for details). The return levels and AGC settings for each collection are provided. These measured parameters were used to calculate the "AGC adjusted voltage" values which were then compared to determine the attenuation levels. The "Baseline" for each collection was used as the reference for each attenuation calculation. Note that the attenuation levels provided are for "two-way" propagation. In other words, the radar signal passed through the precipitation-filled atmospheric medium twice-once on transmission, and once after it was reflected off the target in the scene.

Figure 5-4 illustrates the attenuation levels produced from the various levels and types of precipitation. These attenuation levels have been normalized to 10 meter ranges. These values are not considered substantial; return levels from the FLAR during static collections with precision reference reflectors in a controlled environment have been observed to fluctuate by values approaching these. Note that negative attenuation levels indicate that the peak return from the target in the scene actually increased. This could be due to the wet target causing more of the radar energy to 'be directed back in the direction of the FLAR, or due to the wet ground between the radar and the target causing a higher level of multipath returns.

Table 5-2. Precipitation Test Results

Precipitation Description	Target Range (m)	Measured Return Volts	AGC Control Setting (v)	AGC Mag. Attenuation (dB)	AGC Adjusted Return Volts	Two-Way Power Attenuation (dB)	Two-Way Power Attenuation (dB/10 m)
Light Rain	13	0.492	3.906	-3.6324	0.6064	-0.4	-0.29
Moderate Rain	13	0.441	3.906	-3.6324	0.5436	0.6	0.44
Heavy Rain	13	0.421	3.906	-3.6324	0.5189	1.0	0.75
Moderate Snow	22	0.083	3.906	-3.6324	0.1023	-0.7	-0.30
Heavy Snow	22	0.085	3.906	-3.6324	0.1048	-0.9	-0.39
Fog 1	3	0.366	3.906	-3.6324	0.4511	0.3	1.05
Fog 2	3	0.375	3.906	-3.6324	0.4622	0.1	0.35

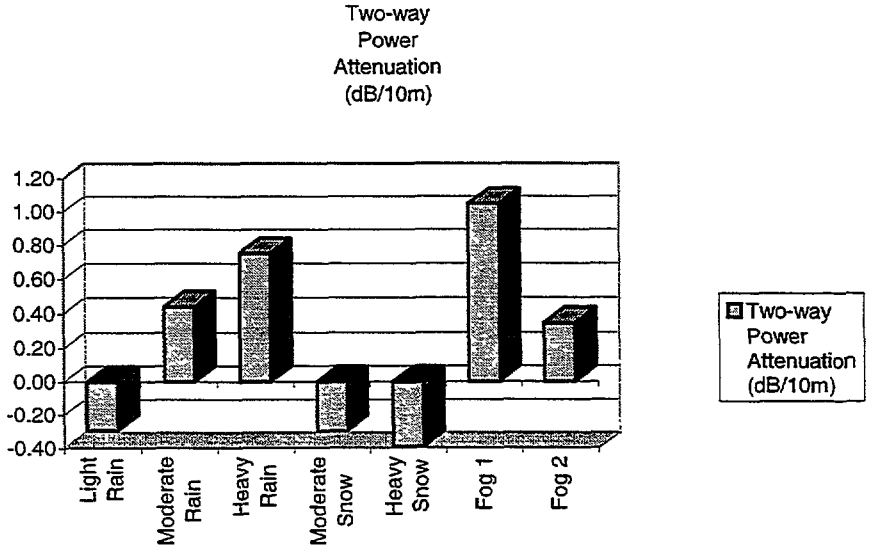

Figure 5-4. Precipitation Attenuation Levels

5.2.2 Conclusions

The primary conclusion of this test is that the FLAR performance was not significantly affected by the various levels and types of precipitation tested. In particular, the precipitation did not produce any observable return levels in the FLAR IF signal, and the attenuation levels were very low. However, the combination of a low RCS target at a far range during heavy rates of precipitation (or heavy fog) could cause a problem for an automotive radar.

The results achieved during this testing correlate well with those in the open literature. There are several papers which have been published on the attenuation of high frequency communication systems as a result of precipitation (see Appendix B). In general, both theoretical and empirical attenuation levels are stated to be about 10 dB per kilometer (one-way). Relating the information obtained in the

open literature to the operating ranges for automotive radars, one could expect power attenuation levels on the order of 1 to 3 dB at 100 meter ranges.

The measurements conducted as part of this program indicate that the actual attenuation levels may be somewhat higher than the 1 to 3 dB values mentioned above. More practical values could range from 2 to 10 dB of power loss at 100 meter ranges. Of course these values are highly dependent upon the rate of precipitation and also particulate size. As the particulate size approaches 1/4 wavelength of the radar frequency, the particulate will begin acting as an antenna.

In practical terms, the most important outcome of this test was the verification that the FLAR was capable of detecting targets within its field-of-view in the presence of significant precipitation. Except for the light rain collections, the target itself was visually obscured from the FLAR's location. During the heavy rain and fog tests, the target was often totally obscured. Despite the visual obscuration, return levels from the target were easily observed in the raw radar signal. These observations provide empirical support to those who cite radar's all-weather performance advantage over infrared or optical sensors for automotive applications.

The surprising phenomenon observed during the testing was the occasional increase in return levels in the presence of precipitation. This was observed during several collections. While the increase was not significant, it was measurable. Possible explanations for this phenomenon are:

- As the precipitation fell, the ground between the radar and the target became wet and a larger multipath return. Theoretically, enhanced multipath returns can increase actual target returns over 10 dB given a particular geometry.
- As the precipitation particles landed in the target, they caused an increase in the non-specular returns due to increased refraction and energy scattering. For tests conducted with reference reflectors, the increase may have come from particles landing on the styrofoam support pedestal.

5.3 CONTAMINATION TESTS

The purpose of these contamination tests was to evaluate how dirt, moisture, and snow would affect the FLAR's performance. The "contamination" could occur either at the target location or at the sensor. For example, the target itself would be considered "contaminated" if it were snow covered, or the sensor could be "contaminated" if its antennas were covered with mud.

The underlying concern for automotive applications is that dirt or other contaminants covering either the target or the sensor itself could severely inhibit the sensor's operation. For example, some laser sensors have had problems tracking targets contaminated with a thick film of dirt.

To evaluate the effect of contaminants on the FLAR, the following contamination scenarios were tested:

- Vehicle target contaminated with snow: In this scenario, the rear portion of the target vehicle (a Pontiac Sunbird) was partially (about 50 percent) covered with fairly dry snow.
- Vehicle target contaminated with water: In this scenario, the target vehicle (a small pick-up truck) was sprayed with water from a hose. Care was taken to perform the baseline test with already wet ground to isolate the vehicle contamination from multipath effects.
- FLAP sensor contaminated with snow: This scenario had approximately 1 inch of snow densely packed on the face of the FLAR sensor.
- FLAB sensor contaminated with semi-dry mud: The mud tests were divided into two levels of contamination- The first level had the glass plate covered with mud, but was still visually translucent. The second level had the glass plate covered with thick mud so that it was visually opaque. This second level is referred to in the tests as "very muddy."

5.3.1 Results

The results of the contamination tests were not what was intuitively expected. Therefore, several data sets were collected/analyzed for each type of test and the results were found to be consistent.

Table 5-3 shows the quantitative summary of the tests. The return levels and AGC settings for each collection are provided. These measured parameters were used to calculate the "AGC adjusted voltage" values which are then compared to determine the attenuation levels. The "Baseline" for each collection was used as the reference for each attenuation calculation. Note that the attenuation levels provided are for "two-way" propagation.

Table 5-3. Contamination Test Summary

Material Description	Measured Return Volts	AGC Control Setting (v)	AGC Mag. Attenuation (dB)	AGC Adjusted Return Volts	Two-Way Power Attenuation (dB)
Water on Truck	0.514	3.906	-3.632	0.634	-0.5
Snow on Car	0.09	3.906	-3.632	0.111	-1.2
Translucent Mud at Sensor	0.197	3.906	-3.632	0.243	-0.7
Opaque Mud at Sensor	0.306	3.906	-3.632	0.377	-4.5
Snow Covered Sensor	0.02	3.906	-3.632	0.025	11.8

Figure 5-5 illustrates the attenuation levels produced from the various types of contamination. Negative attenuation levels indicate that the peak return from the target in the scene actually increased.

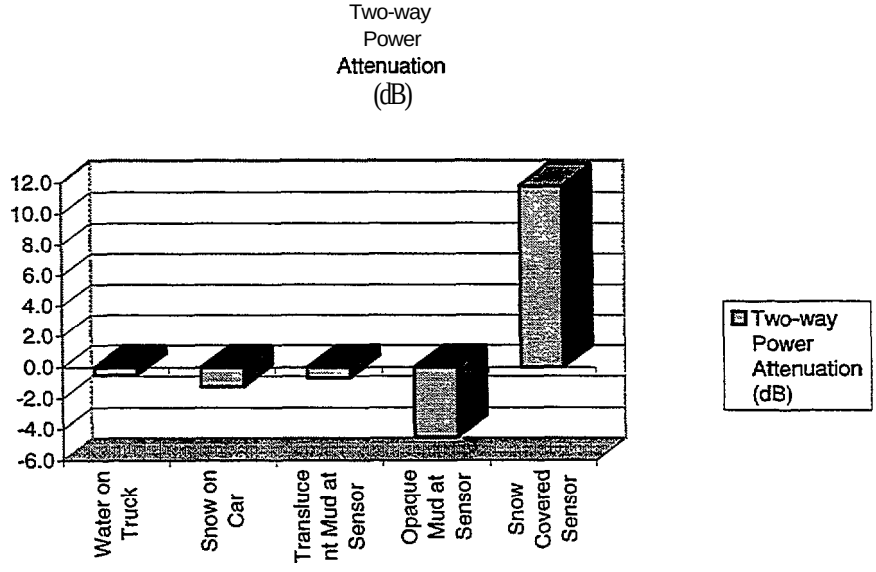

Figure 5-5. Contamination Attenuation Levels

The increases in peak return levels observed in the contaminated vehicle test results correlate with some of the observations made during the precipitation tests. In these cases, a possible explanation is

that the particulate contamination on the vehicle may be enhancing the return level by creating more scattering centers through refraction of the radar energy. See Appendix B for a detailed explanation of this hypothesis.

Results from the contaminated sensor test using semi-dry mud were similar to the contaminated target results. These tests again resulted in 'negative' attenuation, or an observed gain in peak return level. In analyzing the range profiles for the mud contamination tests, it was observed that the contaminated glass plate itself did not reflect energy back to the FLAR. The only difference between the baseline and contamination tests was the peak return level from the reference reflector. A potential cause for this phenomenon is discussed in Appendix B.

Finally, the result of the test in which the FLAR sensor was "caked" with 1 inch of wet snow indicates that the snow did in fact inhibit the sensor from detecting the reference target. Note that the 11 dB signal attenuation caused the reference target return to drop below the system noise level (i.e., the target was not observable).

Special Note: Although these tests indicate a snow-covered vehicle does not pose a detection problem for the radar, the reader should be aware that these results correspond to the specific contamination scenario presented to the FLAR. This scenario was fairly "dry" snow over 50 percent of the rear section of a mid-sized car. We would expect that the heavy "wet" snow which totally covers a vehicle could cause serious detection problems for radar system.

5.3.2 Conclusions

The analyses of the contamination tests have identified some phenomena which were unanticipated. The presence of contamination particulates at both the target and sensor have been observed to cause an increase in the peak return from reference targets in the FLAR's field of view. A potential mechanism for creating this phenomenon is presented in Appendix B. However, it should be noted that this hypothesis has not been thoroughly tested. More research into the phenomenon is required. While the measurement equipment and procedures have been reviewed, the limited access to the FLAR electronics has severely limited our ability to rule out a sensor specific response to the contamination.

The primary conclusion from these tests is that both target and sensor contamination from rain, snow, and mud may cause return levels from targets in the scene to actually increase. This would of course add to the robustness of the automotive radar in detecting objects at non-specular aspect angles. However, the mechanism causing this phenomena needs to be more clearly understood.

Conversely, the snow-covered sensor tests indicate that certain contaminants could also cause severe degradation in sensor performance to the point of missing significant targets within the scene.

6.0 ROADWAY TESTS

The Roadway Tests were conducted in both structured (on test tracks) and unstructured (on freeways) settings. These tests were focused on the sensing issues that might arise in the Adaptive Cruise Control application. To support them a data acquisition and analysis system was developed and upgraded when the prototype radar was upgraded (see Appendix C). In addition, a differential GPS system was developed (see Appendix D) as a truthing tool which provided an independent measurement of the distance between the host vehicle and roadway objects of interest. This system was demonstrated at the 1995 Annual Meeting of ITS America, and at the AVCS Committee Meeting & Vehicle Demonstrations held at the Transportation Research Center (TRC), Inc., East Liberty, Ohio in August, 1996. The structured tests (see Appendix E) were conducted at the TRC in October and November, 1996 in accordance with a test plan developed in cooperation with NHTSA. The detailed test results can be found in Appendix F.

The primary purpose for these tests was to characterize the sensor's measurement performance capabilities in five major categories that are discussed separately in the following sections. Detecting objects, vehicle background, moving or stationary, is a signal processing task that will be addressed from the standpoint of examining the information available from this sensor for detection purposes.

This section will summarize the results and key observations of the structured and unstructured roadway tests. These roadway tests have been grouped into five major categories. The reader should refer to Appendices F and G for more detailed discussion of each of the specific tests.

6.1 BACKGROUND MEASUREMENTS

The issue addressed by these measurements is false alarms that could result from returns induced by "background" objects which include vehicles parked on the roadside, roadside barriers, and vehicles in adjacent lanes.

Table 6- 1 summarizes the results of the various tests which were designed to address the background object/false alarm issue. The information in parentheses following the test title indicates the appendix section in which the tests are discussed in detail. Also, details regarding the test configuration are discussed in the test plan provided in Appendix E.

Table 6- 1. Background Measurements Results and Key Observations

Test Title	Results and Key Observations
Vehicle Induced False Alarms--Straight Roadway-Roadside Vehicle (F.1)	While the FLAR never tracked the roadside vehicles returns from the roadside vehicles were present in the raw radar data at ranges from 50 to 90 meters with the FLAR center beam active. The low return levels (max +3 dBsm for a tractor trailer) are attributed to the orientation between the host and secondary vehicles which causes the roadside vehicle to be illuminated by the low gain fringe of the center beam's mainlobe.
Vehicle Induced False Alarms--Straight Roadway-Adjacent Lane Vehicle (F. 1)	Returns from adjacent lane vehicles were not evident with the FLAR center beam active. Returns in the raw radar data were observed with the left beam active. It was observed that with a tractor/trailer in the adjacent lane, returns were induced by scatterers on both the front and rear portions of the vehicle.
Vehicle Induced False Alarms-Curved Roadway-Roadside Vehicle (F-10)	Guard rails around the outside of a curve induced a characteristic return in the radar as the host vehicle maneuvered through the turn. The returns from the guard rail were significant and the FLAR occasionally "locked-on" to the rail for brief periods of time. Vehicles parked along the curved roadway caused brief returns above those of the guard rail returns *as* the FLAR's center beam scanned across the vehicle. The level of return from the roadside vehicles were significant and varied by type of vehicle. The FLAR processing never "locked on" to any of the roadside vehicles.
Vehicle Induced False Alarms--Curved Roadway-Adjacent Lane Vehicle (F. 10)	Vehicles located in the adjacent lane on a curved roadway were found to induce returns in the raw radar data which are similar to those of a preceding vehicle in the same lane as the host vehicle on a straight roadway. This test scenario clearly indicates that to minimize false alarms, the radar must have some knowledge of the host vehicle dynamics or geometry of the upcoming roadway.
Open Roadway Tests	Bridge overpasses were found to induce substantial returns especially when the issue of vehicle loading was addressed. Tests to evaluate the response to various road surfaces resulted in no observable difference in backsound returns from concrete, asphalt, or dirt roads. Guard rails and roadside signs were observed to induce varying levels of return based on geometric orientation. Hills were found to have little effect in terms of inducing signals in the raw radar data.

6.2 TEMPORAL CHANGES

The issue addressed by these measurements is the ability of the FLAR to respond to traffic changes in terms of the **sensor response time.** Lead vehicle braking either the host or lead vehicle leaving the lane, and cut-ins are all typical roadway events that must be accommodated by the radar sensor. To provide sufficient time for threat assessment algorithm processing driver warning, and driver response, the radar measurement processing latency should be minimized.

Table 6-2 **summarizes** the results of the various tests which were designed to address the temporal change issue. The information in parentheses following the test title indicates the appendix section in which the tests are discussed in detail. Also, details regarding the test configuration are discussed in the test plan provided in Appendix E.

Table 6-2. Temporal Change Measurements Results and Key Observations

Test Title	Results and Key Observations
Braking Secondary Vehicle--Straight Roadway (F.2)	From a system perspective, the FLAR performed-well: accurate tracking of lead vehicle maintained at 20 Hz update rate and the reported range error was consistently < +l meter. From a sensor perspective, the dynamics caused large pulse-to-pulse signal return variations which approached 10 dB.
Intentional Lane Changes--Straight Roadway (F.4)	The radar sensor raw data responded virtually instantaneously to environmental changes. As the host vehicle changed lanes, the returns from the in-lane vehicle did not end abruptly, but dissipated rapidly as the radar beam boresight shifted during the lane change maneuver.
Tracking New Target Vehicle--Straight Roadway (F.5)	During these tests, the FLAR tracking algorithm performed well. As the secondary vehicle changed Ianes, the switch from tracking one vehicle to the other was instantaneous and stable (i.e., no jitter between the tracking of the two vehicles).
Tracking With Cut-In-Straight Roadway (F.6)	The results of these tests were much like those described in F-5 above. The reader is referred to the appendix for a discussion of near range cut-in problems which can occur due to the radar's limited field of view.
Open Roadway Tests	Many temporal changes in medium to heavy traffic scenarios due to dynamic maneuvers, oncoming traffic, and roadside objects were presented to the FLAR. The radar sensor exhibited virtually instantaneous response to the changing conditions, while the FLAR higher-level processing occasionally had some acquisition and tracking latency for new targets. This latency was generally well under 1 second. This illustrates the fact that from a system perspective, the delay in reporting the range to targets and generating track files for threat assessment is highly dependent on filtering and processing algorithms employed.

6.3 RANGE CLUTTER

The issue addressed by these measurements is radar's ability to discriminate between vehicles at various ranges from the host vehicle when the vehicles have significantly different radar cross sections. The vehicle furthest from the host vehicle represents range **clutter** relative to the vehicle immediately in front of the host vehicle (i.e., the secondary vehicle), and could limit the radar's ability to accurately measure the range between the host vehicle and the secondary vehicle.

Table 6-3 summarizes the results of the various tests which were designed to address the range clutter issue. The information in parentheses following the test title indicates the appendix section in which the tests are discussed in detail. Also, details regarding the test configuration are discussed in the test plan provided in Appendix E.

Table 6-3. Range Clutter Measurements Results and Key Observations

Test Title	Results and Key Observations
Strong Vehicle Clutter in Range-Straight Roadway **(F-7)**	The significant observation in this set of tests was that the EAR occasionally lost track of a near range low RCS vehicle (motorcycle) due to the **large** clutter signal from a further range large RCS vehicle (truck). The FLAR was observed to actually start tracking the further range vehicle. This could result in highly undesirable consequences for the ACC application. The range clutter induced errors can be caused by large differences in return levels and reduced radar sensitivity from Automatic **Gain** Control (AGC) activity.
Open Roadway Tests	While the open roadway tests presented the FLAR with a wide variety of traffic scenarios, the FLAR was never observed to lose track of a preceding vehicle due to range clutter returns. Geometries such as those created on the test track were not encountered. This illustrates one of the problems in testing automotive radars, namely, the roadway environment in which the radar must operate is virtually unconstrained with regards to the multitude of geometries and objects which can be encountered. Therefore, careful design and evaluation of potentially problematic scenarios must be carried out under test rack conditions.

6.4 AZIMUTH CLUTTER

The issue addressed by these measurements is radar's ability to discriminate between vehicles in adjacent lanes relative to the host vehicle when the host vehicle is measuring the range to an in-lane secondary vehicle. The vehicles in the adjacent lanesrepresent **azimuth clutter to the** host **vehicle and could** limit the radar's ability to accurately measure the range between the host vehicle and the secondary vehicle. Depending on the nature of the measurement error, the higher-level processing in the ACC system may not be able to reliably track the proper secondary vehicle.

Table 6-4 summarizes the results of the various tests which were designed to address the azimuth clutter issue. The information in parentheses following the test title indicates the appendix **section in** which the tests are discussed in detail. Also, details regarding the test configuration are discussed in the test plan provided **in** Appendix E.

Table 6-4. Azimuth Clutter Measurements Results and Key Observations

Test Title	Results and Key Observations
Out-of-Lane Vehicle Clutter-Straight Roadway, Single Clutter Vehicle (F.3)	Tests conducted with the FLAR center beam activeresulted in no returns from the out-of-iane clutter vehicle. Tests conducted with the FLAR left beam active resulted in low level retnrns from the out-of-lane clutter vehicle. These low level returns did not result in a loss of track on the preceding in-lane vehicle.
Vehicle Clutter in Azimuth-Straight Roadway, Multiple Clutter Vehicles F. 8)	These tests were run with only the FLAR center beam active. No returns from the out-of-lane clutter vehicles were observed. It should be noted that in these tests, the target vehicle maximum range was approximately 50 meters. Higher would result in a wider center beam coverage area which might begin to illuminate adjacent lanes at higher intensities.
Vehicle Clutter in Azimuth-Curved Roadway (F. 12)	Radar returns from both in-lane and adjacent lane vehicles were dependent upon the radius of roadway curvature, range to the vehicles, and boresight of the active antenna. Results showed that instead of tracking the in-lane vehicle, the FLAR tracked the vehicle in the outside lane under commonly encountered geometries. Tests with the left and right FLAR antenna beams active illustrated how "steering" the radar beam while negotiating a curve would enhance the radar sensor's performance with regards to tracking the in-lane vehicle.
Open Roadway Tests	Heavier traffic scenarios actually resulted in few returns from azimuth clutter due to occlusion and AGC sensitivity effects created by near range in-lane objects (heavy traffic density). Tests in lower density traffic showed that azimuth clutter (guard rails, signs, 2-lane oncoming traffic, etc.) cause significant transient returns levels in the raw radar data. The FLAR ACC algorithm never "locked-on" and tracked these returns, however, an algorithm designed for collision avoidance or warning may have false alarm/missed detection problems with these events. It should be noted that systems designed to ignore stationary objects could filter many of these clutter returns out.

6.5 ROADWAY GEOMETRY

Roadway geometry stresses the radar's ability to make range measurements because varying **roadway geometry** essentially requires a wider radar field-of-view to accommodate the angular variations between the host and secondary vehicles. Simply increasing the field-of-view will introduce azimuthal clutter, and thus a basic design trade-off is introduced, that is, simultaneously accommodating varying roadway and traffic conditions.

Table 6-5 summarizes the results of the various tests which were designed to address the roadway geometry issue and its relationship to field-of-view requirements. The information in parentheses following the test title indicates the appendix section in which the tests are discussed in detail. Also, details regarding the test configuration are discussed in the test plan provided in Appendix E.

Table 6-5. Roadway Geometry Measurements Results and Key Observations

Test Title	Results and Key Observations
Merging Traffic-Straight Roadway (F.9)	Roadway geometries associated with merging traffic lanes did NOT induce returns within the FLAR sensor. For these **tests,** the FLAR field-of-view was limited to 3 degrees in azimuth (i.e., the beamwidth of the center transmit antenna). The reader is referred to Section 6.4 ("Azimuth Clutter") for the description of tests which address field-of-view issues for roadside vehicles.
Tracking through a Curve and Vehicle Clutter in Azimuth-Curved Roadway (F.ll and F.12)	These test scenarios are probably the most pertinent to the field-of-view issue. These tests illustrated that the radar sensor field-of-view must be wider than 3 degrees to effectively track in-lane objects beyond a 20 meter **range** on a typical roadway curvature. The reader should also refer to test scenario F. 10 ("Vehicle Induce False Alarms-Curved Roadway") for a discussion on the impact of guard rails around curves and the relationship with sensor field-of-view.
Open Roadway Tests	The open roadway tests in medium to heavy traffic scenarios were somewhat encouraging in that they showed occlusion and AGC sensitivity effects from the higher traffic densities effectively reduced the radar's field-of-view by limiting its range. In these cases, the reduced field-of-view did not inhibit tracking the preceding in-lane vehicle throughout a variety of road geometries and provided the benefit in eliminating much of the out-of-lane clutter. However, light traffic tests showed how azimuthal clutter from numerous objects generate significant transient radar returns which must be addressed by processing algorithms. Many of these returns were from objects such as guardrails and roadside signs located on curved roadways. Also, a variety of hills were encountered in the open roadway tests which were found not to induce any significant returns in the FLAR sensor. The biggest impact on the hills was the loss of track on the preceding in-lane vehicle for low traffic densities.

7.0 SUMMARY

This section will summarize the findings and conclusions of the FLAR program.

7.1 CHARACTERIZATION OF VEHICLES AND ROADWAY OBJECTS

ERIM's Fine Resolution Rotary Platform Imaging Facility was used to create radar images of selected roadway objects. The roadway objects were selected to provide a meaningful set of data across a variety of objects which could be commonly found in a roadway environment. To that end, data was collected on the following objects:

- 1990 Chevy Corvette ZR-1
- 1995 Ford Taurus
- 1991 Jeep Wrangler
- 1993 Geo Metro
- Honda Motorcycle
- Human
- Stop Sign
- Cinder Block Wall

Data for each of the objects listed above was collected by a 94 GHz instrumentation radar. The object was rotated while being illuminated by the radar so that reflection characteristics of the object which are angle dependent could be identified. The radar data was processed to create two-dimensional images of each object. The images are useful in identifying the parts of the object which are and are not reflective to the radar energy for a given aspect angle.

In addition to the images, the radar data was processed to produce radar cross-section values for each object. The radar cross-section, or RCS, is a quantitative value which describes the object's level of radar reflectivity. The data collected supports analyzing RCS both as function of aspect angle and as a function of range across the target.

Section 3 of this final report provides a detailed description of both the image and digital data outputs available as a result of the database creation. The reader is also referred to Appendix A which includes a general discussion of radar cross-section and its dependence on object material, object shape, and aspect angle.

In general, the critical information available in the database can be divided into three categories: (1) maximum and minimum RCS values, (2) dependency of RCS on object shape or aspect angle, and (3) distribution of radar reflectors on a given object.

First, examining the data across all the objects which were measured, indicates that RCS levels vary from around +40 dBsm for a broadside perspective of a Jeep, to -2 dBsm for a motorcycle, down to - 10 dBsm for a stop sign. Furthermore, besides varying from object to object, the RCS can vary greatly for a single object depending upon aspect angle. For example, the RCS for the Jeep ranged from a maximum of +40 dBsm down to well below +5 dBsm. This wide variation plays a significant role in the development of radar sensor hardware which must have enough sensitivity to detect small RCS targets in the presence of large RCS targets.

Second, observations of maximum RCS as a function of aspect angle illustrates how an object's shape affects its radar reflectivity. For example, a relatively square Taurus-type vehicle exhibits a significant decrease in RCS as its aspect angle departs from 180 degrees (180 degrees is defined as

viewing a target from behind-&at is, looking at a vehicle's rear end). On the other hand, a more curved vehicle like a Corvette or Metro, exhibited less of an abrupt fall-off in RCS as the aspect angle departed from 180 degrees. These characteristics can be related to the ability of an automotive radar to track a given vehicle through a roadway curve. Again, knowledge of the extent of RCS changes as a function of aspect angle are valuable to a sensor designer in terms of addressing sensitivity issues.

Third, the images which were produced by the RCS database work provide valuable insight into the attributes of an object which actually cause the radar reflectivity. The images illustrated the distribution of radar reflectors (a.k.a. scatterers) across a target. In particular, the impact of side-view mirrors, wheels, under-body structures (e.g., transmission housing), and even body panel seams are evident. Knowledge of these radar scattering mechanisms is critical for radar processing and threat assessment algorithm developers. For example, the ability to identify multiple scatterers as part of a single object will have a major impact on the load placed on the processing electronics.

In summary, this effort established an initial database which could support the efforts of hardware designers, algorithm developers, and simulation programmers. The database's value to hardware designers and algorithm developers has already been discussed. However, its greatest utility may come in the form of support to collision avoidance system simulation programs. The simulation programs can make use of the data to apply range and aspect angle dependent RCS attributes to objects within the simulation scene.

Since the establishment of the database, information has been made available to interested parties in the form of hard copy images and data plots as well as digital data files. Hard copies of the data images and plots have been compiled into a "Catalog of Radar Scattering Characteristics for Common Roadway Objects." Hard copies of the database information is available through NHTSA-OCAR and the digital data files can be downloaded from ERIM's website (http:\www.erim-int.com).

Finally, additional discussion of the database can be found in the technical paper:

- "Millimeter Wave Scattering Characteristics and Radar Cross Section Measurement of Common Roadway Objects," P.K. Zoratti, J.J. Ference, R. Majewski, and R.K. Gilbert. In ***Proceedings of the SPIE on Collision Avoidance and Automated Traffic Management Sensors,*** Philadelphia, PA, 25-26 October 1995. Vol. 2592

7.2 ROADWAY TESTS

When one considers the number of different types of situations which may be presented to an automotive radar, a combinatoric explosion of possibilities is encountered. Obviously it was not practical to attempt evaluating the FLAR performance under all possible conditions. Instead, a series of tests was designed to evaluate the FLAR performance in some standard roadway settings and also some settings in which it was anticipated that the FLAR performance may be degraded. The primary variables for the tests included: (1) roadway geometry (e.g., straight, curved, sloped); (2) background clutter (e.g., out of path vehicles, guard rails, roadside signs); and (3) location and density of other moving vehicles on the roadway. The complete test plan is provided in Appendix E of this report.

The tests were conducted on both a closed test track and the open roadway. To evaluate the sensor performance during the road tests, the ERIM testbed vehicle acquired a variety of data including the raw radar signal (i.e., the IF signal), the TRW processed data (e.g., range and range rate of object being tracked), and video data of the road scene. In addition, a differential GPS system was used on several of the tests to independently locate the position of a target vehicle with respect to the FLAR sensor. Information on the DGPS truthing solution and its accuracy is provided in a paper in Appendix D of this report.

It is important to note that in interpreting the test results, one must take care in differentiating between the sensor performance and the system performance. The sensor performance pertains to the radar sensor itself and how it interacts with a given roadway environment. The system performance pertains to how the raw radar data is interpreted by the processing electronics and algorithms to depict the actual state of the environment within the sensor's field of view. The FLAR sensor used in these tests was developed by TRW for an Adaptive Cruise Control (ACC) type of application. Therefore, the sensor as well as the processing algorithms was designed specifically for the ACC application which has different requirements than a collision warning application. The real purpose of the tests conducted in this project was to focus on the sensor performance, but when appropriate, the overall TRW FLAR system performance was also analyzed.

The results from the various road scenarios tested are summarized in Section 6. A more complete discussion of each test conducted on the closed test track is provided in Appendix F. The data collections made on the open roadway are discussed in Appendix G. Both appendices include numerous data plots illustrating the sensor response to the specific test scenario. Where appropriate, quantitative calculations are provided. The analysis presented in Appendices F and G are is focused primarily on the radar sensor performance perspective. The objective of this analysis was to identify particular scenarios which could result in a raw radar data response which could prove difficult to interpret by standard processing and threat assessment algorithms.

The scenarios identified as potential problems are summarized below. ***(Note that these results must be taken in the context of the FLAR configuration which had 3 switched antennas with 3 degree azimuth and 3 degree elevation beam widths. Sensors with different configuration can have significantly different performance.):***

- **Roadside vehicles on a straight roadway** were observed to generate returns in the raw radar data at certain geometries which could be interpreted as objects within the host vehicle's lane.
- **Adjacent lane vehicles on a straight roadway** viewed by on the FLAR side beam antennas can generate multiple returns with significant range separation.
- **Guard rails and other roadside objects** on **curved roadways** generated significant returns which could cause false alarm problems.
- **Tracking vehicles around curved roadways** could prove to be problematic without knowledge of the roadway geometry in front of the sensor.
- **Near-range cut-ins and tracking of narrow vehicles** such as motorcycles could cause missed detections due to limited radar field-of-view.
- **Low RCS vehicles located between radar and large RCS vehicles** could cause missed detections.
- **Bridge or other roadway** overpasses were observed to generate significant returns in the raw radar data under certain circumstances.

In general, the radar sensor itself performed very well in the roadway tests. Somewhat counter-intuitive was the fact that the FLAR performed well under heavier traffic densities than under very light traffic densities. This was a result of a decreased amount of clutter returns due to limiting the sensor's field-of-view by the near range traffic. The response time of the raw radar data signal to changes in the roadway environment was virtually instantaneous given the 7 millisecond pulse repetition rate. For example, objects which were present in the radar's field-of-view for only a short duration, such as a parked vehicle on the roadside in a curve, were easily identified in the raw radar data. Two areas of the sensor configuration were identified as critical to achieving adequate roadway performance: (1) antenna design and control, and (2) receiver gain control.

The FLAR radar antenna beam width and side lobe levels define the radar's field-of-view at any given instant. While the side lobe levels were not attributed to any shortcomings in the radar performance, the roadway tests in this program indicated that the FLAR's 3 degree azimuth beam width may be too wide to reduce the effect of azimuth clutter to an acceptable level. For instance, vehicles parked on the roadside on a straight roadway induced radar returns which could possibly be interpreted as a low RCS object located in the center of the roadway. Also, it was identified that the FLAR would have problems tracking the appropriate vehicle around a curve without knowledge of the roadway geometry.

A number of automotive radar developers are addressing these shortcomings by using a narrower beam antenna which is scanned across the desired field-of-view. By correlating the radar response in one scan position with the response to another scan position, objects should be able to be placed much more accurately in a azimuth plane. This will work well for azimuth clutter on a straight roadway, but it appears that some knowledge of the roadway geometry preceding the host vehicle must be available to the processing algorithms in order to adequately handle tracking vehicles through a curve. The ability to "steer" the radar beam in a curve is highly desirable. Of course a scanned narrow beam antenna can add significant cost, real-estate requirements, and processing complexity.

The other area of sensor configuration which was identified as critical was the receiver gain control. The RCS data collected as part of this program indicates that objects may vary by as much as 40 dBsm or more. In order to achieve this dynamic range, the FLAR sensor employs a variable gain amplifier with the receiver electronics. When a large signal level is detected with the FLAR receiver, the gain of the amplifier is decreased. This can lead to the undesired situation where a large RCS target at some medium range, say a truck at 40 meters, can reduce the sensitivity of the radar such that a low RCS target at some near range, say a motorcycle at 20 meters, is not detected.

The extension of the basic radar sensor performance to the higher level system functionality for ACC and CWS applications becomes manifested in "false alarms" and "missed detections." From the tests conducted under this program, it was concluded that except for the limitations sited above, the FLAR sensor performs fairly well from the pure radar perspective. That is, the raw radar data responds to its environment in an acceptable manner. The success of applying the radar sensor to ACC and CWS lies in the interpretation (i.e., processing) of the radar data in such a way as to produce an acceptable level of false alarms and missed detections.

The roadway tests and their resulting data identified a number of scenarios which need to be addressed by the processing algorithms to be employed by ACC and CWS applications. The primary issue is the timely assessment of whether or not a detected object causes a real threat to the host vehicle. Systems which purposely ignore returns from stationary objects will have a much easier task in assessing threats, however, their value as a collision warning sensor will certainly be limited. Assuming that detection and assessment of stationary objects is necessary means that all the returns from the roadway "clutter" must be properly identified.

The returns which result from a guard rail as a vehicle enters a curve is a good example of a scenario which needs to be addressed by the threat assessment algorithm. Analyzing the raw radar data without knowledge of the roadway environment could lead to the conclusion that there is a stopped object within the host vehicle lane. Depending upon the timing thresholds of a CWS, this scenario could generate a false alarm. Data collected under this program shows a characteristic signature which develops from the guard rail as the host vehicle maneuvers through the turn. Knowledge of this signature, combined with information about the road geometry in front of the host vehicle and perhaps some knowledge of the azimuthal extent of the guard rail would allow a much more robust threat assessment algorithm to be employed. The empirical data collected during this program also indicates that roadside signs and oncoming traffic pose similar problems.

7.3 TESTING, EVALUATION AND CERTIFYING METHODOLOGIES

During this program a number of testing and evaluation methods were identified and used to evaluate the FLAR performance. In addition, the empirical data produced by the RCS and roadway measurements will support the creation of future "controlled" test procedures which can be repeated to refine an automotive radar's performance both in terms of configuration and processing.

To begin with the FLAR sensor had to be characterized via laboratory type measurements to support the analysis of roadway data. This laboratory characterization included measuring the range accuracy, range resolution, and field-of-view of the radar sensor. These types of measurements will need to be made to validate the typical performance specifications of the unit as claimed by the manufacturer. Section 4 of this report provides details on the tests conducted and their results.

During the laboratory testing, several anomalies in the FLAR's performance were identified and explained. For example, the range accuracy of the FLAR was found to decrease with increased distance. This error was attributed to the FLAR' s linear FM modulation rate (i.e., chirp rate) being slightly different than that specified by TRW. This was not surprising since the RF electronics within the sensor can have variability due to manufacturing, temperature, and age. The point to make is that procedures for calibrating the operation of automotive radar's must be developed to insure accurate performance.

After characterizing the baseline performance of the FLAR, the sensor was subjected to a number of different environmental conditions in terms of precipitation, material occlusion, and radome/target contamination. The results of these tests are provided in Section 5. The results of these tests is significant in terms of comparing radar technology to other types of remote sensing alternatives. As expected, the radar performed very well under precipitation tests which is the primary advantage of radar over infrared and laser sensing systems- The materials test served to identify the type of material which could be used to house the radar sensor as well as which materials could pose detection problems for radar.

Beyond laboratory calibration procedures and environmental sensitivities of the FLAR sensor, this program identified some common roadway scenarios which could cause erroneous performance. In addition to identifying the scenarios, the data collected also provides quantitative information which can be used to develop measurable and repeatable test procedures for validation of system performance.

For example, the open roadway tests conducted to evaluate the impact of bridge overpasses indicates that for a host vehicle to operate adequately with 5 degrees of tilt due to loading the rear compartment, the sensor must be able to reject the equivalent returns from a 2.5 dBsm object located approximately 14 feet above the roadway with a large azimuthal extent. Note that this problem statement defines several parameters around which a standardized roadway test can be created. With this type of empirical data, a test track can be outfitted with calibrated targets positioned properly to represent a given roadway scenario.

Besides generating the empirical data sited above, this program also validated the use of a differential GPS solution to serve as a truthing mechanism for specially orchestrated dynamic roadway testing.

In addition to actual physical testing of the radar sensor, the data produced by the RCS measurements database created under this program will support the simulation' testing of collision warning sensors. While a number of problematic roadway scenarios were identified during the roadway testing effort of this program, it was not possible to subject the FLAR to the extremely large number of combinatoric roadway scenario possibilities. Also, safety of the test engineers and drivers limited the types of orchestrated maneuvers which could be conducted. For these reasons, simulation testing of well modeled sensors and targets is still necessary.

7.4 CONCLUDING REMARKS

In summary, the foundation for generating a series of tests to validate the performance of an automotive radar has been produced by this program. This series of tests includes laboratory calibration, evaluation of environmental performance, repeatable roadway testing using calibrated reflectors to represent a roadway scenario, and the use of simulation.

To conclude this report, several areas related to collision warning and adaptive cruise control system development which warrant further investigation will be cited.

Expansion of RCS Database

There has been a high level of interest from system developers in the RCS database since its creation. This database consists of a limited number of objects all collected at a single range under benign weather conditions. Expansion of the database to include a more diverse set of objects under varying environmental conditions should be explored to support future sensor development and simulation programefforts.

Mutual Interference

This program focused on the response of the FLAR sensor to a variety of roadway scenarios. However, these roadway scenarios did not have any other radar sensors present. Susceptibility to mutual interference is highly dependent upon sensor confirmation. As these sensors are introduced into the automotive market and their penetration increases, the mutual interference among sensors may become an issue. Both physical and simulation techniques can be used to evaluate what level of impact mutual interference may have on widespread system operational use.

Manufacturing, Installation. and Calibration Issues

If FLAR-type sensors are to be mass produced and factory installed on vehicles, issues regarding sensor calibration must be addressed. For example, to what degree will an installation tolerance of +1 degree of sensor alignment affect system performance? Should the sensor be self-aligning? To what extent will the aging of the signal generation electronics affect system accuracy? If a host vehicle gets bumped in the parking lot and throws the system out of alignment, should the system detect the problem and notify the operator?

These types of issues are obviously far-reaching and sensor-dependent, however, some basic research in this area may affect sensor design to address these issues.

Use of Simulation to Test Sensor Design and Algorithm Implementation

Due to safety and the number of combinatoric roadway scenario possibilities, simulation of collision warning sensors may prove invaluable in the sensor design and algorithm implementation process. For example, one roadway scenario which was not tested as part of this program is the near-range cut-in. In this scenario an adjacent lane vehicle would enter the host vehicle's lane at a range of less than 5 meters. This scenario poses problems for an automotive radar with limited field-of-view. This scenario was not tested in this program due to safety concerns for the drivers. However, appropriately modeled simulation programs could address this and other dangerous scenarios and allow for sensor performance evaluation.

Human Factors and Response to Nuisance Alarms

Work related to the acceptable level of nuisance or false alarms would provide a valuable threshold benchmark to which automotive radar systems could be designed.

Human Factors and Response to Avoidance Maneuvers

To take collision safety to the ultimate level, collision sensors may someday initiate avoidance maneuvers. Basic research on the types and severity of maneuvers which are acceptable to the vehicle operator is necessary before any such system is implemented.